Corrected Article: "An error-controlled fast multipole method" [J. Chem. Phys. 131, 244102 (2009)]

Holger Dachsel

Citation: The Journal of Chemical Physics **132**, 119901 (2010); doi: 10.1063/1.3358272
View online: https://doi.org/10.1063/1.3358272
View Table of Contents: http://aip.scitation.org/toc/jcp/132/11
Published by the American Institute of Physics

Publisher's Note: The original article was published in the 28 December 2009 issue with several incorrectly broken equations and spacing problems around the "!" symbols in the formulas. AIP apologizes for these errors. The article republished here is unchanged from the original published version except for the breaks in some mathematical expressions and the spacing around the "!" symbols in the formulas. This article should be cited as Holger Dachsel, J. Chem. Phys. **132**, 119901 (2010).

Corrected Article: "An error-controlled fast multipole method" [J. Chem. Phys. 131, 244102 (2009)]

Holger Dachsel[a)]
Institute for Advanced Simulation, Jülich Supercomputing Centre, Forschungszentrum Jülich, 52425 Jülich, Germany

(Received 12 December 2008; accepted 27 October 2009; published online 16 March 2010)

We present a two-stage error estimation scheme for the fast multipole method (FMM). This scheme can be applied to any particle system. It incorporates homogeneous as well as inhomogeneous distributions. The FMM error as a consequence of the finite representation of the multipole expansions and the operator error is correlated with an absolute or relative user-requested energy threshold. Such a reliable error control is the basis for making reliable simulations in computational physics. Our FMM program on the basis of the two-stage error estimation scheme is available on request. © *2010 American Institute of Physics*. [doi:10.1063/1.3358272]

I. INTRODUCTION

The fast multipole method (FMM)[1–5] is one of the most effective methods to evaluate pairwise potentials required in several scientific applications such as molecular dynamics[6] and plasma physics.[7] The FMM achieves linear scaling with respect to the number of particles by expanding local charges in multipole expansions and can be applied to a variety of potentials. The control of the errors due to the finite expansions is a crucial aspect in the application of the FMM.[4,8–11] Any error estimation dealing with the worst case scenario with respect to the positions of the particles in the boxes and the distance between the boxes always overestimates the length of these expansions. The basis of a reliable error estimation scheme is the computation of a small upper error limit. The smaller this limit can be computed the better is the error estimation scheme. The scheme should include the contributions of all particles to the FMM error. Using the approach described in this paper the level of poles depending on a user-requested energy threshold can be determined. Because our error estimation scheme follows the FMM algorithm in detail we do not need to apply Chebyshev polynomials. Chebyshev economization always assumes the worst case scenario. Such a situation is certainly not the case for a realistic particle distribution. The Chebyshev economization only includes the errors resulting from the truncation of the infinite expansion of the reciprocal distance. In the FMM approach further errors are incurred by use of the operator **B**.[4,5] These errors are ignored by the Chebyshev economization.

Besides the operator **B** (multipole-to-local translation) the FMM uses the operators **A** (multipole-to-multipole translation) and **C** (local-to-local translation). The FMM could also be implemented without the use of the operators **A** and **C** increasing the complexity from $\mathcal{O}(N)$ to $\mathcal{O}(N \log N)$. However, the two different implementations give the exact same results. Because we must use a finite binary floating point representation the results of the schemes only differ within the magnitude of the machine precision. The use of the operators **A** and **C** has no impact on the accuracy of the calculation (energy, potential, and gradient).[3] The operators **A** and **C** translate exact up to the level of poles in the unshifted expansions. Because **A** and **C** have no impact on the accuracy of the results these operators do not affect the errors. Hence, the operators **A** and **C** do not need to be considered in the FMM error estimation scheme. Therefore only operator **B** has to be taken into account as described in this paper. The error due to the finite representation of the multipole expansions is implicitly handled in our scheme.

This work has been motivated by the requirements of numerical simulations in the field of laser plasma interaction.[12–16] Simulations of clusters consisting of 10^6 or more charged particles simply require a reliable error control for various reasons. Due to error accumulation, hundreds of thousands or millions of time steps within a molecular dynamics simulation could lead to unphysical artifacts. Without error control a small change in the geometry of a single particle could cause a discontinuous change in the energy in case the particle moves from its original box to another box on a certain level of the FMM tree.

The basic idea of our FMM error estimation scheme is to compute the errors depending on the actual particle positions. Assuming the worst case scenario always overestimates the level of poles. Our approach determines a smaller level of poles for a certain user-requested energy threshold. It can reduce the total runtime of a FMM calculation by an order of magnitude or even more.

[a)]Electronic mail: h.dachsel@fz-juelich.de.

The development of a reliable and effective error estimation scheme for the FMM is in principle not an easy subject and therefore a certain level of mathematics is necessary to tackle this problem. Nevertheless we have tried to keep the mathematics as simple as possible following the notation used by White and Head-Gordon.[4,5] We have implemented the two-stage error estimation scheme described in this paper in our FMM program which is available on request.[17]

A. Laser plasma interaction

The interaction of clusters with intensive ($>10^{15}$ W/cm^2) and short (≤ 1 ps) laser pulses is one of the frontiers in physics today. Very interesting phenomena can be investigated, for example, the formation of highly charged ions and high energetic electrons. The irradiation of clusters with intensive short laser pulses shows many fascinating dynamical phenomena, starting with the mechanisms of energy absorption from the laser pulse and ending with the process of recombination when the cluster expands. High-energy Coulomb explosion of clusters caused by femtosecond pulses has been observed. For large clusters, strong laser pulses could even create a nanocluster inside the cluster. Reliable computer simulations of intensive laser pulse interactions with plasma targets are the key to understand these processes. All these phenomena are the result of effective energy absorption from the laser field into the cluster. The energy absorption leads to a rapid expansion of the cluster on a femtosecond time scale. In the course of expansion the electron density decreases resulting in strong energy absorption. The explosion of clusters ejects for example xenon ions with kinetic energies up to 1 MeV. Compared to the Coulomb explosion of molecules this energy is about four orders of magnitude higher. The laser-induced Coulomb explosion of clusters shows that access to an extremely high temperature state of matter is possible, which is the basis for fusion experiments.

II. THEORY

In order to derive the algorithm we assume the particle coordinates are scaled so that all particles are enclosed by a box with a coordinate range from 0 to 1 in each spatial direction. We propose a two-stage error estimation scheme. In the first stage homogeneous distributions of particles in all boxes on all levels of the FMM tree are assumed. In the second stage the real distributions of the particles in the boxes are taken into account by using an additional space domain decomposition for each box. Hence, the contribution of each particle with respect to the absolute or relative energy error is taken into account. It shows that the error contribution of a single particle depends strongly on the distance of the particle to the center of the box.

A. First stage of the error estimation scheme

At first we compute an average absolute error of the interactions of two separated boxes with respect to the level of poles p, at which the multipole expansions are truncated. We average over all possible box positions depending on the FMM separation criterion ws.[4] The energy of two separated

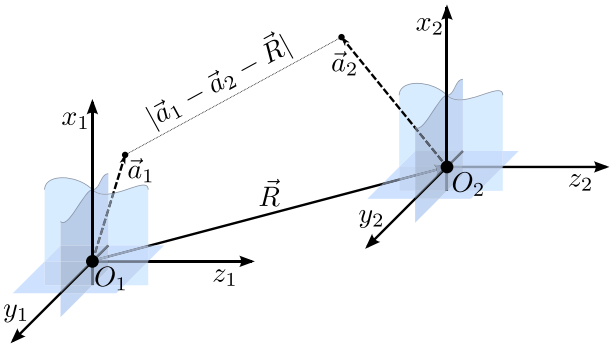

FIG. 1. The positions of the two box centers. Subscript 1 refers to box 1 and subscript 2 to box 2, respectively.

boxes[18] (Fig. 1) within the rotation based FMM[4,5,19–21] approach can be written in complete form as follows:

$$E = \sum_{l=0}^{\infty} \sum_{m=-l}^{l} \sum_{j=0}^{\infty} \sum_{k=-j}^{j} \sum_{n=-\min(j,\,l)}^{\min(j,\,l)} (-1)^j \times \sqrt{\frac{(l-m)!(l+m)!}{(l-n)!(l+n)!}} e^{im\phi} d^l_{mn}(\theta) \omega^{\text{box 1}}_{lm} \frac{(j+l)!}{R^{j+l+1}} \times \sqrt{\frac{(j-k)!(j+k)!}{(j-n)!(j+n)!}} e^{ik\phi} d^j_{k,\,-n}(\theta) \omega^{\text{box 2}}_{jk}. \quad (1)$$

The variables R, θ, and ϕ are the spherical coordinates with respect to the relative position of the two box centers to each other. The matrices d^l and d^j are components of the Wigner D-matrices.[19–21] The summation over n in Eq. (1)

$$\sum_{n=-\min(j,\,l)}^{\min(j,\,l)} \sqrt{\frac{(l-m)!(l+m)!}{(l-n)!(l+n)!}} d^l_{mn}(\theta) \times \sqrt{\frac{(j-k)!(j+k)!}{(j-n)!(j+n)!}} d^j_{k,\,-n}(\theta) = \frac{(j+l-k-m)!}{(j+l)!} P_{j+l,\,k+m}(\cos(\theta)) \quad (2)$$

is leading to the energy expression of the conventional FMM which is a better approach for an error estimation scheme compared to Eq. (1). The energy of the conventional FMM is given by

$$E = \sum_{l=0}^{\infty} \sum_{m=-l}^{l} \sum_{j=0}^{\infty} \sum_{k=-j}^{j} (-1)^j \omega^{\text{box 1}}_{lm} \times \frac{(j+l-k-m)!}{R^{j+l+1}} P_{j+l,\,k+m}(\cos(\theta)) e^{i(k+m)\phi} \omega^{\text{box 2}}_{jk}. \quad (3)$$

The terms $P_{j+l,\,k+m}$ are the associated Legendre polynomials. The multipole moments of the two boxes are defined by $\omega^{\text{box 1}}_{lm}$ and $\omega^{\text{box 2}}_{jk}$ with

$$\omega^{\text{box 1}}_{lm} = \sum_{I=1}^{N^{\text{box 1}}} q_I a_I^l \frac{1}{(l+m)!} P_{lm}(\cos(\alpha_I)) e^{-im\beta_I} \quad (4)$$

and

$$\omega_{jk}^{\text{box }2} = \sum_{J=1}^{N^{\text{box }2}} q_J a_J^j \frac{1}{(j+k)!} P_{jk}(\cos(\alpha_J)) e^{-ik\beta_J}. \tag{5}$$

The upper bounds $N^{\text{box }1}$ and $N^{\text{box }2}$ indicate the number of particles in the two boxes. q_I is the charge of particle I, and a_I, α_I, and β_I are the spherical coordinates of particle I with respect to the center of the first box. q_J is the charge of particle J, and a_J, α_J, and β_J are the spherical coordinates of particle J with respect to the center of the second box. Now we can compute the upper limit for the multipole moments of a homogeneous distribution. The absolute value of the phase factors is equal to 1

$$|e^{-im\beta_I}| = 1, \tag{6}$$

$$|e^{-ik\beta_J}| = 1. \tag{7}$$

To avoid any under- and overflows in the binary floating point representations we substitute the terms $1/(l+m)!$ by $l!/(l+m)!$ in Eq. (4) and $1/(j+k)!$ by $j!/(j+k)!$ in Eq. (5) and introduce the terms 2^{-l} and 2^{-j}. We introduce the averaged multipole moments for level L $(L>0)$ of the FMM tree as follows

$$\tilde{\omega}_{lm}^{\text{box }1} = \left(\sum_{I=1}^{N^{\text{box }1}} |q_I|\right) \frac{\int_{-1}^{1}\int_{-1}^{1}\int_{-1}^{1} \left(\frac{\sqrt{x^2+y^2+z^2}}{2\times 2^L}\right)^l \frac{l!}{(l+m)!} \left| P_{lm}\left(\frac{z}{\sqrt{x^2+y^2+z^2}}\right)\right| dxdydz}{\int_{-1}^{1}\int_{-1}^{1}\int_{-1}^{1} dxdydz}. \tag{8}$$

The value $L=1$ corresponds to the complete simulation box $[0,\ldots,1,\ 0,\ldots,1,\ 0,\ldots,1]$. Due to symmetry Eq. (8) can be simplified

$$\tilde{\omega}_{lm}^{\text{box }1} = (2^{-L})^l \left(\sum_{I=1}^{N^{\text{box }1}} |q_I|\right) \int_0^1\int_0^1\int_0^1 \left(\frac{\sqrt{x^2+y^2+z^2}}{2}\right)^l \times \frac{l!}{(l+m)!} \left| P_{lm}\left(\frac{z}{\sqrt{x^2+y^2+z^2}}\right)\right| dxdydz. \tag{9}$$

We obtain the analog expression for the multipole moments of the second box

$$\tilde{\omega}_{jk}^{\text{box }2} = (2^{-L})^j \left(\sum_{J=1}^{N^{\text{box }2}} |q_J|\right) \int_0^1\int_0^1\int_0^1 \left(\frac{\sqrt{x^2+y^2+z^2}}{2}\right)^j \times \frac{j!}{(j+k)!} \left| P_{jk}\left(\frac{z}{\sqrt{x^2+y^2+z^2}}\right)\right| dxdydz. \tag{10}$$

The introduction of the two chargeless multipole moments

$$\tilde{\tilde{\omega}}_{lm} = \int_0^1\int_0^1\int_0^1 \left(\frac{\sqrt{x^2+y^2+z^2}}{2}\right)^l \times \frac{l!}{(l+m)!} \left| P_{lm}\left(\frac{z}{\sqrt{x^2+y^2+z^2}}\right)\right| dxdydz \tag{11}$$

and

$$\tilde{\tilde{\omega}}_{jk} = \int_0^1\int_0^1\int_0^1 \left(\frac{\sqrt{x^2+y^2+z^2}}{2}\right)^j \times \frac{j!}{(j+k)!} \left| P_{jk}\left(\frac{z}{\sqrt{x^2+y^2+z^2}}\right)\right| dxdydz \tag{12}$$

is leading to

$$\tilde{\omega}_{lm}^{\text{box }1} = (2^{-L})^l \left(\sum_{I=1}^{N^{\text{box }1}} |q_I|\right) \tilde{\tilde{\omega}}_{lm} \tag{13}$$

and

$$\tilde{\omega}_{jk}^{\text{box }2} = (2^{-L})^j \left(\sum_{J=1}^{N^{\text{box }2}} |q_J|\right) \tilde{\tilde{\omega}}_{jk}. \tag{14}$$

The integration can be performed numerically with sufficient accuracy. We have used the Romberg integration method. The box with coordinate ranges $[0,\ldots,1,\ 0,\ldots,1,\ 0,\ldots,1]$ is divided in half along each Cartesian axis ten times to yield 8^{10} boxes, respectively, 8^{10} points have been used in the numerical integration. We have performed the numerical integration in double precision (64 bits for the representation of a floating point number). The distance R in Eq. (3) represents the distance between the centers of two separated boxes. Each level L of the FMM tree consists of 2^{L-1} boxes in one dimension (1D). To obtain a level-independent distance $\tilde{R}$ we define

$$\tilde{R} = 2^L R. \tag{15}$$

On each level we have 8^{L-1} boxes in three dimensions (3D). The distance $\tilde{R}$ is always equal to or greater than $2(ws+1)$ and less than or equal to $2(2ws+1)\sqrt{3}$ in case separated boxes exist on the level L. To guarantee numerical stability we rearrange terms and use normalized associated Legendre polynomials. We introduce the term

$$\frac{(j+l)!}{j!l!2^{j+l+1}} \tag{16}$$

with $j+l>0$ for the purpose of correction. This term corresponds to a probability and compensates the overestimation of the level of poles p as a consequence of the disregard of

the real distribution of positive and negative contributions, since we treat negative contributions as being positive. The summation over j in Eq. (16) is always unity

$$\sum_{j=0}^{\infty} \frac{(j+l)!}{j!l!2^{j+l+1}} = 1. \tag{17}$$

The absolute value of the phase factor in Eq. (3) is equal to 1

$$|e^{i(k+m)\phi}| = 1. \tag{18}$$

Now we use Eqs. (9), (10), (15), (16), and (18) to simplify Eq. (3) yielding

$$\tilde{E}_L = 2^{L-1}\tilde{E} \tag{19}$$

with

$$\begin{aligned}\tilde{E} = {} & 2\frac{\tilde{\omega}_{00}^{\text{box 1}}\tilde{\omega}_{00}^{\text{box 2}}}{\tilde{R}} \\ & + \sum_{l=0}^{\infty}\sum_{m=-l}^{l}\sum_{j=0}^{\infty}\sum_{k=-j}^{j}\frac{\tilde{\omega}_{lm}^{\text{box 1}}}{(2^{-L})^l}\left(\frac{2(ws+1)}{\tilde{R}}\right)^{j+l+1} \\ & \times\frac{\sqrt{(j+l-k-m)!(j+l+k+m)!}}{j!l!(ws+1)^{j+l+1}} \\ & \times\frac{(j+l)!}{j!l!2^{j+l+1}}|P_{j+l,\ |k+m|}^{\text{normalized}}(\cos(\theta))|\frac{\tilde{\omega}_{jk}^{\text{box 2}}}{(2^{-L})^j},\quad j+l>0.\end{aligned} \tag{20}$$

The normalized associated Legendre polynomials are given by

$$\begin{aligned}P_{j+l,\ |k+m|}^{\text{normalized}}(\cos(\theta)) = {} & \sqrt{\frac{(j+l-|k+m|)!}{(j+l+|k+m|)!}} \\ & \times P_{j+l,\ |k+m|}(\cos(\theta))\end{aligned} \tag{21}$$

with

$$|P_{j+l,\ |k+m|}^{\text{normalized}}(\cos(\theta))| \le 1. \tag{22}$$

For now we neglect the charges and use Eqs. (13) and (14) to simplify Eq. (20)

$$\begin{aligned}\tilde{E} = {} & 2\frac{\tilde{\tilde{\omega}}_{00}\tilde{\tilde{\omega}}_{00}}{\tilde{R}} + \sum_{l=0}^{\infty}\sum_{m=-l}^{l}\sum_{j=0}^{\infty}\sum_{k=-j}^{j}\tilde{\tilde{\omega}}_{lm} \\ & \times\left(\frac{2(ws+1)}{\tilde{R}}\right)^{j+l+1}\frac{\sqrt{(j+l-k-m)!(j+l+k+m)!}}{j!l!(ws+1)^{j+l+1}} \\ & \times\frac{(j+l)!}{j!l!2^{j+l+1}}|P_{j+l,\ |k+m|}^{\text{normalized}}(\cos(\theta))|\tilde{\tilde{\omega}}_{jk},\quad j+l>0\end{aligned} \tag{23}$$

with

$$\tilde{\tilde{\omega}}_{00} = \int_0^1\int_0^1\int_0^1 dxdydz = 1 \tag{24}$$

and average over all possible box-box interactions. By taking into account all the eight child boxes of a certain box and neglecting edge effects we have to consider $56(2ws+1)^3$ box-box interactions. Each interaction is defined by a pair of spherical coordinates $(R_i,\ \theta_i)$. Some of these interactions may be defined by the same pair of spherical coordinates. We define

$$\tilde{\tilde{E}} = \sum_{l=0}^{\infty}\sum_{j=0}^{\infty} g_{jl} \tag{25}$$

with

$$g_{00} = \frac{2\tilde{\tilde{\omega}}_{00}\tilde{\tilde{\omega}}_{00}}{56(2ws+1)^3}\sum_{i=1}^{56(2ws+1)^3}\frac{1}{\tilde{R}_i} \tag{26}$$

and

$$\begin{aligned}g_{jl} = {} & \frac{1}{56(2ws+1)^3}\sum_{i=1}^{56(2ws+1)^3}\sum_{m=-l}^{l}\sum_{k=-j}^{j}\tilde{\tilde{\omega}}_{lm} \\ & \times\left(\frac{2(ws+1)}{\tilde{R}_i}\right)^{j+l+1}\frac{\sqrt{(j+l-k-m)!(j+l+k+m)!}}{j!l!(ws+1)^{j+l+1}} \\ & \times\frac{(j+l)!}{j!l!2^{j+l+1}}|P_{j+l,\ |k+m|}^{\text{normalized}}(\cos(\theta_i))|\tilde{\tilde{\omega}}_{jk},\quad j+l>0.\end{aligned} \tag{27}$$

The elements of g_{jl} satisfy the symmetry condition $g_{jl}=g_{lj}$. Since FMM implementations demand a finite level of poles p causing an error in Eq. (1), p can be obtained by splitting the two sums in Eq. (25) into two parts, a sum from 0 to p and a second sum from $p+1$ to infinity, yielding

$$\tilde{\tilde{E}} = \sum_{l=0}^{p}\left(\sum_{j=0}^{p} g_{jl} + \sum_{j=p+1}^{\infty} g_{jl}\right) + \sum_{l=p+1}^{\infty}\left(\sum_{j=0}^{p} g_{jl} + \sum_{j=p+1}^{\infty} g_{jl}\right). \tag{28}$$

Now we obtain the error for $\tilde{\tilde{E}}$ as a function of the level of poles p with

$$\begin{aligned}\Delta\tilde{\tilde{E}}(p) = {} & \sum_{l=0}^{p}\sum_{j=p+1}^{\infty} g_{jl} + \sum_{l=p+1}^{\infty}\sum_{j=0}^{p} g_{jl} + \sum_{l=p+1}^{\infty}\sum_{j=p+1}^{\infty} g_{jl} \\ = {} & \sum_{l=0}^{p}\sum_{j=p+1}^{\infty} g_{jl} + \sum_{l=p+1}^{\infty}\sum_{j=0}^{\infty} g_{jl}.\end{aligned} \tag{29}$$

The vector $\Delta\tilde{\tilde{E}}$ can be pre-computed and stored (Table I). The function $\Delta\tilde{\tilde{E}}(p)$ is shown in Fig. 2. The precomputed values can be used in a simulation as follows. After the particle coordinates have been scaled, the parent box is divided into eight child boxes in 3D. Each of these child boxes is subdivided creating 64 child boxes in 3D on level 3. This procedure continues until the minimum of computation time has been found depending on a user-requested absolute energy threshold ΔE_{req}. On each level of the FMM tree with separated boxes all far field box-box interactions

TABLE I. $\Delta\tilde{\tilde{E}}$ depending on the level of poles for $0 \leq p \leq 101$.

Level of poles	$\Delta\tilde{\tilde{E}}$
0	$0.346\,731\,006\,239\,123\,069 \times 10^{-01}$
1	$0.562\,465\,411\,713\,349\,089 \times 10^{-02}$
2	$0.116\,936\,137\,039\,975\,664 \times 10^{-02}$
3	$0.286\,323\,285\,926\,225\,595 \times 10^{-03}$
4	$0.790\,774\,393\,858\,241\,045 \times 10^{-04}$
5	$0.240\,199\,453\,480\,825\,078 \times 10^{-04}$
6	$0.790\,161\,568\,817\,730\,142 \times 10^{-05}$
7	$0.277\,794\,622\,043\,420\,435 \times 10^{-05}$
8	$0.103\,448\,891\,695\,808\,980 \times 10^{-05}$
9	$0.405\,586\,188\,452\,373\,622 \times 10^{-06}$
10	$0.166\,697\,913\,065\,686\,554 \times 10^{-06}$
11	$0.714\,180\,324\,616\,708\,230 \times 10^{-07}$
12	$0.318\,405\,206\,475\,023\,056 \times 10^{-07}$
13	$0.146\,925\,468\,839\,778\,159 \times 10^{-07}$
14	$0.700\,209\,322\,516\,717\,622 \times 10^{-08}$
15	$0.343\,711\,670\,713\,892\,661 \times 10^{-08}$
16	$0.173\,192\,977\,463\,490\,001 \times 10^{-08}$
17	$0.894\,389\,839\,347\,706\,292 \times 10^{-09}$
18	$0.471\,856\,157\,766\,461\,623 \times 10^{-09}$
19	$0.253\,885\,659\,792\,516\,785 \times 10^{-09}$
20	$0.139\,155\,853\,271\,036\,045 \times 10^{-09}$
21	$0.774\,806\,428\,149\,775\,649 \times 10^{-10}$
22	$0.437\,973\,100\,288\,791\,631 \times 10^{-10}$
23	$0.250\,897\,959\,392\,884\,788 \times 10^{-10}$
24	$0.145\,521\,280\,136\,111\,869 \times 10^{-10}$
25	$0.853\,959\,295\,135\,225\,828 \times 10^{-11}$
26	$0.506\,093\,274\,942\,549\,819 \times 10^{-11}$
27	$0.302\,909\,206\,303\,276\,927 \times 10^{-11}$
28	$0.182\,932\,728\,104\,287\,674 \times 10^{-11}$
29	$0.111\,368\,947\,775\,526\,674 \times 10^{-11}$
30	$0.683\,381\,017\,661\,747\,299 \times 10^{-12}$
31	$0.422\,176\,848\,863\,055\,456 \times 10^{-12}$
32	$0.262\,622\,690\,729\,507\,371 \times 10^{-12}$
33	$0.164\,399\,252\,291\,339\,076 \times 10^{-12}$
34	$0.103\,482\,028\,019\,455\,833 \times 10^{-12}$
35	$0.655\,143\,170\,259\,656\,972 \times 10^{-13}$
36	$0.416\,831\,809\,049\,214\,025 \times 10^{-13}$
37	$0.266\,521\,344\,937\,552\,025 \times 10^{-13}$
38	$0.171\,208\,773\,767\,498\,294 \times 10^{-13}$
39	$0.110\,431\,360\,494\,495\,074 \times 10^{-13}$
40	$0.715\,461\,231\,109\,113\,583 \times 10^{-14}$
41	$0.465\,244\,430\,656\,835\,537 \times 10^{-14}$
42	$0.303\,644\,668\,125\,161\,447 \times 10^{-14}$
43	$0.198\,914\,450\,784\,026\,232 \times 10^{-14}$
44	$0.130\,717\,619\,978\,435\,692 \times 10^{-14}$
45	$0.861\,930\,118\,736\,359\,871 \times 10^{-15}$
46	$0.569\,974\,113\,554\,490\,419 \times 10^{-15}$
47	$0.378\,005\,643\,922\,669\,805 \times 10^{-15}$
48	$0.251\,463\,748\,423\,698\,124 \times 10^{-15}$
49	$0.167\,681\,532\,448\,788\,446 \times 10^{-15}$
50	$0.112\,109\,725\,775\,368\,340 \times 10^{-15}$
51	$0.751\,378\,604\,546\,538\,147 \times 10^{-16}$
52	$0.504\,772\,887\,241\,145\,989 \times 10^{-16}$
53	$0.339\,940\,944\,384\,364\,819 \times 10^{-16}$
54	$0.229\,357\,612\,857\,324\,952 \times 10^{-16}$
55	$0.155\,090\,896\,652\,443\,053 \times 10^{-16}$
56	$0.105\,095\,591\,428\,024\,057 \times 10^{-16}$
57	$0.713\,464\,542\,506\,227\,146 \times 10^{-17}$
58	$0.485\,325\,100\,928\,894\,121 \times 10^{-17}$
59	$0.330\,661\,108\,107\,414\,281 \times 10^{-17}$
60	$0.225\,712\,315\,521\,735\,834 \times 10^{-17}$
61	$0.154\,348\,299\,847\,622\,816 \times 10^{-17}$
62	$0.105\,697\,803\,772\,035\,782 \times 10^{-17}$
63	$0.725\,091\,247\,693\,815\,271 \times 10^{-18}$
64	$0.498\,120\,238\,571\,297\,246 \times 10^{-18}$
65	$0.342\,715\,886\,198\,196\,062 \times 10^{-18}$
66	$0.236\,154\,871\,564\,270\,836 \times 10^{-18}$
67	$0.162\,924\,997\,003\,520\,526 \times 10^{-18}$
68	$0.112\,577\,672\,081\,913\,740 \times 10^{-18}$
69	$0.778\,812\,242\,668\,708\,876 \times 10^{-19}$
70	$0.539\,442\,806\,730\,615\,923 \times 10^{-19}$
71	$0.374\,171\,963\,549\,876\,115 \times 10^{-19}$
72	$0.259\,810\,755\,348\,535\,438 \times 10^{-19}$
73	$0.180\,633\,222\,470\,452\,024 \times 10^{-19}$
74	$0.125\,714\,489\,266\,537\,428 \times 10^{-19}$
75	$0.875\,877\,390\,705\,820\,314 \times 10^{-20}$
76	$0.611\,037\,835\,707\,714\,833 \times 10^{-20}$
77	$0.426\,639\,056\,089\,346\,960 \times 10^{-20}$
78	$0.298\,202\,942\,920\,053\,238 \times 10^{-20}$
79	$0.208\,641\,456\,061\,492\,213 \times 10^{-20}$
80	$0.146\,118\,188\,762\,707\,277 \times 10^{-20}$
81	$0.102\,444\,609\,383\,165\,003 \times 10^{-20}$
82	$0.718\,750\,343\,683\,977\,255 \times 10^{-21}$
83	$0.504\,759\,144\,853\,701\,595 \times 10^{-21}$
84	$0.354\,829\,073\,547\,639\,235 \times 10^{-21}$
85	$0.249\,619\,957\,112\,292\,326 \times 10^{-21}$
86	$0.175\,773\,128\,342\,598\,693 \times 10^{-21}$
87	$0.123\,857\,021\,460\,654\,878 \times 10^{-21}$
88	$0.873\,510\,914\,198\,504\,058 \times 10^{-22}$
89	$0.616\,587\,698\,251\,202\,001 \times 10^{-22}$
90	$0.435\,489\,807\,308\,156\,787 \times 10^{-22}$
91	$0.307\,857\,569\,061\,083\,891 \times 10^{-22}$
92	$0.217\,778\,185\,552\,155\,634 \times 10^{-22}$
93	$0.154\,164\,756\,334\,168\,359 \times 10^{-22}$
94	$0.109\,218\,091\,210\,508\,913 \times 10^{-22}$
95	$0.774\,178\,267\,063\,568\,442 \times 10^{-23}$
96	$0.549\,225\,992\,133\,482\,842 \times 10^{-23}$
97	$0.389\,869\,364\,369\,932\,214 \times 10^{-23}$
98	$0.276\,906\,016\,944\,480\,070 \times 10^{-23}$
99	$0.196\,825\,617\,009\,790\,711 \times 10^{-23}$
100	$0.139\,975\,734\,381\,477\,048 \times 10^{-23}$
101	$0.996\,159\,298\,985\,506\,144 \times 10^{-24}$

$(\Sigma_{K(L)}\Sigma_{M(K)})$ have to be taken into account. Finally we have to sum over all levels L and all box-box interactions on the levels

$$\Delta E_{\text{req}} \geq \frac{1}{2}\Delta\tilde{\tilde{E}}(p)\sum_{L}\sum_{K(L)}\sum_{M(K)} 2^{L-1}\left(\sum_{I=1}^{N^{\text{box}\ K}} |q_I|\right) \times\left(\sum_{J=1}^{N^{\text{box}\ M}} |q_J|\right). \tag{30}$$

Because each box-box interaction is computed twice we have to divide the result by 2. We can change Eq. (30) slightly to be computationally more efficient

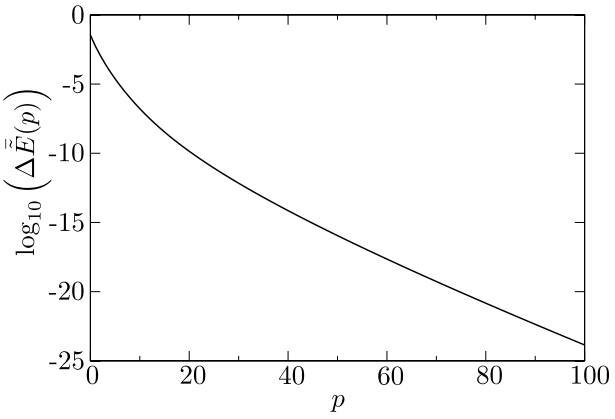

FIG. 2. $\log_{10}(\Delta\tilde{\tilde{E}})$ as a function of the level of poles.

$$\Delta E_{\text{req}} \geq \Delta\tilde{\tilde{E}}(p)\sum_{L}\sum_{K(L)}\sum_{M(K)>K} 2^{L-1}\left(\sum_{I=1}^{N^{\text{box}\ K}}|q_I|\right)\times\left(\sum_{J=1}^{N^{\text{box}\ M}}|q_J|\right). \tag{31}$$

Now each box-box interaction is computed once only. Finally Eq. (31) is used to find the smallest possible value for p. The determined value of p is always correct for systems consisting of homogeneously or nearly homogeneously distributed particles. Depending on the user-requested absolute energy threshold it is also possible to neglect the entire far field contribution. Therefore we can define an interval for the ratio of the exact far field energy E assuming all charges being either positive or negative and the monopole approximation E_0 of E by

$$c_1 \leq \frac{E}{E_0} \leq c_2 \tag{32}$$

with

$$c_1 = 2 \min_{i=-2ws-1}^{2ws+1}\min_{j=-2ws-1}^{2ws+1}\min_{k=-2ws-1}^{2ws+1}\min_{-2\leq g_i\leq 2}\min_{-2\leq g_j\leq 2}\min_{-2\leq g_k\leq 2} \sqrt{\frac{i^2+j^2+k^2}{(2i+g_i)^2+(2j+g_j)^2+(2k+g_k)^2}}, \quad \max(|i|,\ |j|,\ |k|) > ws \tag{33}$$

and

$$c_2 = 2 \max_{i=-2ws-1}^{2ws+1}\max_{j=-2ws-1}^{2ws+1}\max_{k=-2ws-1}^{2ws+1}\max_{-2\leq g_i\leq 2}\max_{-2\leq g_j\leq 2}\max_{-2\leq g_k\leq 2} \sqrt{\frac{i^2+j^2+k^2}{(2i+g_i)^2+(2j+g_j)^2+(2k+g_k)^2}}, \quad \max(|i|,\ |j|,\ |k|) > ws. \tag{34}$$

In case ws is equal to 1, $c_1=\sqrt{6/17}$ and $c_2=\sqrt{6}$ (Fig. 3). The limit of c_1 and c_2 is given by

$$\lim_{ws\to\infty} c_1 = \lim_{ws\to\infty} c_2 = 1. \tag{35}$$

Finally we can write

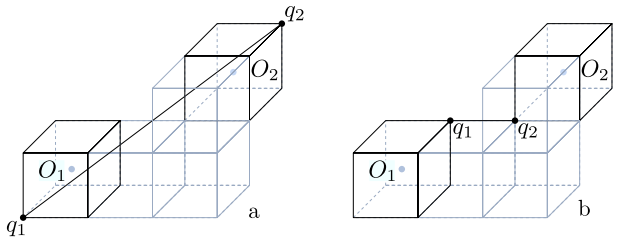

FIG. 3. The minimal and maximal ratio E/E_0 of the exact far field energy E and the monopole approximation E_0 of E for $ws=1$. The minimal ratio $\sqrt{6/17}$ is illustrated in (a). The maximal ratio $\sqrt{6}$ is illustrated in (b). The charges q_1 and q_2 are located in box 1 with origin O_1 and box 2 with origin O_2, respectively.

$$\sqrt{6/17} \leq c_1 \leq 1, \qquad 1 \leq c_2 \leq \sqrt{6}. \tag{36}$$

The terms c_1 and c_2 are strictly monotonic increasing, respectively, decreasing with respect to ws (Fig. 4). The terms c_1 and c_2 for $1\leq ws\leq 10$ are shown in Table II.

The monopole approximation E_0 of the far field energy E is defined by

$$E_0 = \frac{1}{2}\sum_{L}\sum_{K(L)}\sum_{M(K)} \frac{\left(\Sigma_{I=1}^{N^{\text{box}\ K}}|q_I|\right)\left(\Sigma_{J=1}^{N^{\text{box}\ M}}|q_J|\right)}{|\mathbf{R}_K-\mathbf{R}_M|} = \sum_{L}\sum_{K(L)}\sum_{M(K)>K} \frac{\left(\Sigma_{I=1}^{N^{\text{box}\ K}}|q_I|\right)\left(\Sigma_{J=1}^{N^{\text{box}\ M}}|q_J|\right)}{|\mathbf{R}_K-\mathbf{R}_M|}. \tag{37}$$

$\mathbf{R}_K=(x_K,y_K,z_K)^T$ and $\mathbf{R}_M=(x_M,y_M,z_M)^T$ are the coordinates of the box centers. We can neglect the far field contribution to the energy completely in case

$$\Delta E_{\text{req}} \geq c_2 E_0. \tag{38}$$

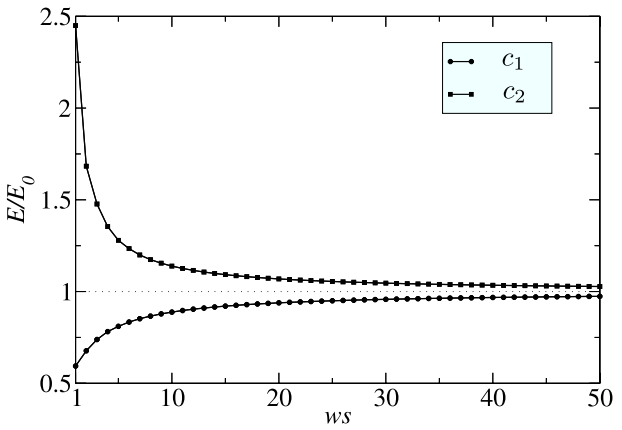

FIG. 4. The terms c_1 and c_2 as functions of ws.

TABLE II. The terms c_1 and c_2 for $1 \le ws \le 10$.

ws	c_1	c_2
1	0.594 088 525 786 004 585	2.449 489 742 783 178 098
2	0.677 003 200 386 330 030	1.683 250 823 060 346 326
3	0.738 548 945 875 996 396	1.477 097 891 751 992 793
4	0.781 735 959 970 571 592	1.354 006 400 772 660 060
5	0.810 380 415 552 132 998	1.279 204 298 133 662 606
6	0.833 739 738 299 376 129	1.233 988 360 045 293 429
7	0.851 858 977 069 655 170	1.199 415 062 114 891 975
8	0.866 025 403 784 438 647	1.173 903 224 498 427 246
9	0.878 203 752 021 909 479	1.154 700 538 379 251 529
10	0.888 065 196 826 467 797	1.138 687 915 757 221 612

B. Second stage of the error estimation scheme

Now we can go a step further to improve our scheme. After we have set up the FMM tree to achieve the minimum of computation time (subject of a next paper) assuming a homogeneous distribution, the positions of all particles must not be changed anymore. Now we can include the actual distributions of particles in all boxes on all levels of the FMM tree in the second stage of our error estimation scheme. This procedure is necessary because the individual error contribution of a single particle strongly depends on its position in the box with respect to the box center. In general two particles with the same charge contribute very differently to the energy error in case the first particle is located near the box center and the second one is located far away from the center in one of the box corners.

To derive the second stage lets consider the far field interaction of two separated boxes. We obtain an upper error limit if we incorporate only the largest of the three distances d_x, d_y, and d_z with

$$d_x = |x_{\text{center}}^{\text{box } 1} - x_{\text{center}}^{\text{box } 2}|, \tag{39}$$

$$d_y = |y_{\text{center}}^{\text{box } 1} - y_{\text{center}}^{\text{box } 2}|, \tag{40}$$

$$d_z = |z_{\text{center}}^{\text{box } 1} - z_{\text{center}}^{\text{box } 2}|, \tag{41}$$

$$d = \max(d_x,\ d_y,\ d_z). \tag{42}$$

On a certain level of the FMM tree the distance d can take $ws+1$ different values. For the sake of clarity we substitute d by R. Without loss of generality we can assume the two boxes are located along the Z axis. The box centers are separated by the distance d [Eq. (42)]. After we have chosen d, any rotations about the X, Y, or Z axis by a rotation angle of $k(\pi/2)$(k integer) must be without any relevance with respect to the quantity of the error.

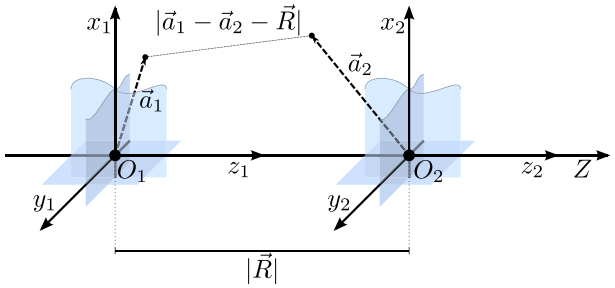

FIG. 5. The positions of the two box centers along the Z axis. Subscript 1 refers to box 1 and subscript 2 to box 2, respectively.

The energy of two separated boxes located along the Z axis[18] (Fig. 5) is given by

$$E = \sum_{l=0}^{\infty}\sum_{j=0}^{\infty}\sum_{m=-\min(j,\ l)}^{\min(j,\ l)} (-1)^{j+m}\omega_{lm}^{\text{box } 1}(+1)^{j+l}\frac{(j+l)!}{R^{j+l+1}}(\omega_{jm}^{\text{box } 2})^*$$
$$= \sum_{l=0}^{\infty}\sum_{j=0}^{\infty}\sum_{m=-\min(j,\ l)}^{\min(j,\ l)} (-1)^{j+m}\omega_{lm}^{\text{box } 2}(-1)^{j+l}\frac{(j+l)!}{R^{j+l+1}}(\omega_{jm}^{\text{box } 1})^*. \tag{43}$$

The asterisk in Eq. (43) symbolizes the conjugate-complex of $\omega_{jm}^{\text{box } 2}$ and $\omega_{jm}^{\text{box } 1}$, respectively. By now we ignore the charges and the sum over all particles in the multipole moments. The chargeless versions of the multipole moments are given by

$$\omega_{lm}^{\text{box } 1} = a_1^l \frac{1}{(l+m)!}P_{lm}(\cos(\alpha_1))e^{-im\beta_1} \tag{44}$$

and

$$\omega_{jm}^{\text{box } 2} = a_2^j \frac{1}{(j+m)!}P_{jm}(\cos(\alpha_2))e^{-im\beta_2}. \tag{45}$$

Now we replace the chargeless multipole moments in Eq. (43) using Eqs. (44) and (45) and rearrange terms

$$E = \frac{1}{R}\sum_{l=0}^{\infty}\sum_{j=0}^{\infty}\sum_{m=-\min(j,\ l)}^{\min(j,\ l)} (-1)^{j+m}\left(\frac{a_1}{R}\right)^l \frac{l!}{(l+m)!}P_{lm}(\cos(\alpha_1))e^{-im\beta_1}(+1)^{j+l}\left(\frac{a_2}{R}\right)^j \frac{j!}{(j+m)!}P_{jm}(\cos(\alpha_2))e^{im\beta_2}\frac{(j+l)!}{j!l!}$$
$$= \frac{1}{R}\sum_{l=0}^{\infty}\sum_{j=0}^{\infty}\sum_{m=-\min(j,\ l)}^{\min(j,\ l)} (-1)^{j+m}\left(\frac{a_2}{R}\right)^l \frac{l!}{(l+m)!}P_{lm}(\cos(\alpha_2))e^{-im\beta_2}(-1)^{j+l}\left(\frac{a_1}{R}\right)^j \frac{j!}{(j+m)!}P_{jm}(\cos(\alpha_1))e^{im\beta_1}\frac{(j+l)!}{j!l!}. \tag{46}$$

To derive an expression for the energy error we reformulate Eq. (46)

$$E=\frac{1}{2R}\sum_{l=0}^{\infty}\sum_{j=0}^{\infty}\sum_{m=-\min(j,\ l)}^{\min(j,\ l)}\left((-1)^{j+m}\left(\frac{a_1}{R}\right)^{l}\frac{l!}{(l+m)!}P_{lm}(\cos(\alpha_1))e^{-im\beta_1}(+1)^{j+l}\left(\frac{a_2}{R}\right)^{j}\frac{j!}{(j+m)!}P_{jm}(\cos(\alpha_2))e^{im\beta_2}\frac{(j+l)!}{j!l!}\right.$$
$$\left.+(-1)^{j+m}\left(\frac{a_2}{R}\right)^{l}\frac{l!}{(l+m)!}P_{lm}(\cos(\alpha_2))e^{-im\beta_2}(-1)^{j+l}\left(\frac{a_1}{R}\right)^{j}\frac{j!}{(j+m)!}P_{jm}(\cos(\alpha_1))e^{im\beta_1}\frac{(j+l)!}{j!l!}\right). \tag{47}$$

Now we can split the first two sums in Eq. (47)

$$\sum_{l=0}^{\infty}\sum_{j=0}^{\infty}\cdots=\sum_{l=0}^{p}\sum_{j=0}^{p}\cdots+\sum_{l=0}^{p}\sum_{j=p+1}^{\infty}\cdots+\sum_{l=p+1}^{\infty}\sum_{j=0}^{p}\cdots+\sum_{l=p+1}^{\infty}\sum_{j=p+1}^{\infty}\cdots. \tag{48}$$

Using Eqs. (47) and (48) we obtain an error for the energy E

$$\Delta E=\frac{1}{R}\sum_{l=0}^{p}\sum_{j=p+1}^{\infty}\sum_{m=-l}^{l}\left((-1)^{j+m}\left(\frac{a_1}{R}\right)^{l}\frac{l!}{(l+m)!}P_{lm}(\cos(\alpha_1))e^{-im\beta_1}(+1)^{j+l}\left(\frac{a_2}{R}\right)^{j}\frac{j!}{(j+m)!}P_{jm}(\cos(\alpha_2))e^{im\beta_2}\frac{(j+l)!}{j!l!}\right.$$
$$\left.+(-1)^{j+m}\left(\frac{a_2}{R}\right)^{l}\frac{l!}{(l+m)!}P_{lm}(\cos(\alpha_2))e^{-im\beta_2}(-1)^{j+l}\left(\frac{a_1}{R}\right)^{j}\frac{j!}{(j+m)!}P_{jm}(\cos(\alpha_1))e^{im\beta_1}\frac{(j+l)!}{j!l!}\right)$$
$$+\frac{1}{2R}\sum_{l=p+1}^{\infty}\sum_{j=p+1}^{\infty}\sum_{m=-\min(j,\ l)}^{\min(j,\ l)}\left((-1)^{j+m}\left(\frac{a_1}{R}\right)^{l}\frac{l!}{(l+m)!}P_{lm}(\cos(\alpha_1))e^{-im\beta_1}(+1)^{j+l}\left(\frac{a_2}{R}\right)^{j}\frac{j!}{(j+m)!}P_{jm}(\cos(\alpha_2))e^{im\beta_2}\frac{(j+l)!}{j!l!}\right.$$
$$\left.+(-1)^{j+m}\left(\frac{a_2}{R}\right)^{l}\frac{l!}{(l+m)!}P_{lm}(\cos(\alpha_2))e^{-im\beta_2}(-1)^{j+l}\left(\frac{a_1}{R}\right)^{j}\frac{j!}{(j+m)!}P_{jm}(\cos(\alpha_1))e^{im\beta_1}\frac{(j+l)!}{j!l!}\right). \tag{49}$$

To make Eq. (49) more manageable we consider only the terms for $0\le l\le p+1$ and change the summation sequence

$$\Delta E=\frac{1}{R}\sum_{l=0}^{p}\sum_{m=-l}^{l}\sum_{j=p+1}^{\infty}\left((-1)^{j+m}\left(\frac{a_1}{R}\right)^{l}\frac{l!}{(l+m)!}P_{lm}(\cos(\alpha_1))e^{-im\beta_1}(+1)^{j+l}\left(\frac{a_2}{R}\right)^{j}\frac{j!}{(j+m)!}P_{jm}(\cos(\alpha_2))e^{im\beta_2}\frac{(j+l)!}{j!l!}\right.$$
$$\left.+(-1)^{j+m}\left(\frac{a_2}{R}\right)^{l}\frac{l!}{(l+m)!}P_{lm}(\cos(\alpha_2))e^{-im\beta_2}(-1)^{j+l}\left(\frac{a_1}{R}\right)^{j}\frac{j!}{(j+m)!}P_{jm}(\cos(\alpha_1))e^{im\beta_1}\frac{(j+l)!}{j!l!}\right)$$
$$+\frac{1}{2R}\sum_{l=p+1}^{p+1}\sum_{m=-l}^{l}\sum_{j=p+1}^{\infty}\left((-1)^{j+m}\left(\frac{a_1}{R}\right)^{l}\frac{l!}{(l+m)!}P_{lm}(\cos(\alpha_1))e^{-im\beta_1}(+1)^{j+l}\left(\frac{a_2}{R}\right)^{j}\frac{j!}{(j+m)!}P_{jm}(\cos(\alpha_2))e^{im\beta_2}\frac{(j+l)!}{j!l!}\right.$$
$$\left.+(-1)^{j+m}\left(\frac{a_2}{R}\right)^{l}\frac{l!}{(l+m)!}P_{lm}(\cos(\alpha_2))e^{-im\beta_2}(-1)^{j+l}\left(\frac{a_1}{R}\right)^{j}\frac{j!}{(j+m)!}P_{jm}(\cos(\alpha_1))e^{im\beta_1}\frac{(j+l)!}{j!l!}\right). \tag{50}$$

For reasons of simplicity we drop the term

$$(-1)^{j+m}\left(\frac{a_2}{R}\right)^{l}\frac{l!}{(l+m)!}P_{lm}(\cos(\alpha_2))e^{-im\beta_2}(-1)^{j+l}\left(\frac{a_1}{R}\right)^{j}\frac{j!}{(j+m)!}P_{jm}(\cos(\alpha_1))e^{im\beta_1}\frac{(j+l)!}{j!l!} \tag{51}$$

in both triple sums in Eq. (50) but later on we have to take it into account as well. We neglect all the remaining terms with $l>p+1$ in Eq. (49). Now we perform the summation step by step starting with $l=0$ which gives our first error contribution of zeroth order with respect to l

$$\Delta E_{l=0}=\frac{1}{R}\left|\sum_{j=p+1}^{\infty}(\pm1)^{j}\left(\frac{a_2}{R}\right)^{j}P_{j0}(\cos(\alpha_2))\right|. \tag{52}$$

The conventional approach is to take the absolute value of the product $(\pm1)^{j}P_{j0}(\cos(\alpha_2))$ and set $|P_{j0}(\cos(\alpha_2))|$ to 1. It certainly provides an upper limit for $\Delta E_{l=0}$ but the summation of positive and negative terms to achieve a smaller upper error limit is unconsidered and the level of poles p is overestimated with respect to a user-requested energy threshold. Following the conventional approach we can easily compute the infinite sum in Eq. (52) yielding

$$\Delta E_{l=0}\le\frac{1}{R-a_2}\left(\frac{a_2}{R}\right)^{p+1}. \tag{53}$$

To assign Eq. (53) a practical meaning we have to assume the worst case scenario which means the particle is located in one of the box corners and the two boxes are separated by

the smallest possible distance. Such a situation is certainly not the case for the majority of the particles. Therefore the level of poles p is overestimated even more. A better and by far a more practical approach is to apply the absolute value as late as possible and to incorporate error terms of higher order. Our scheme proceeds as follows. We apply a space domain decomposition in one of the interacting boxes. We divide this box into 8^5 grid boxes obtaining 32^3 grid points at the centers of the grid boxes. We include additional grid points on each coordinate axis yielding a total of 33^3 grid points. Now we compute the sum in Eq. (52) for each grid point and for $(-1)^j$ and $(+1)^j$ separately, take the maximum and store the values $F_{0p}(a_2,\ \alpha_2)$ as constants in a library

$$F_{0p}(a_2,\ \alpha_2) = \max_{s=-1,\ 1} \left| \sum_{j=p+1}^{\infty} s^j \left(\frac{a_2}{R}\right)^j P_{j0}(\cos(\alpha_2)) \right|. \quad (54)$$

After computing the error contribution of zeroth order we proceed with the first order error contribution. The error term of the first order $\Delta E_{l=1}$ depends on the coordinates of both particles and is given by

$$\begin{aligned}\Delta E_{l=1} = \frac{c_1}{R}\left(\frac{a_1}{R}\right) \Bigg| & P_{10}(\cos(\alpha_1)) \sum_{j=p+1}^{\infty} (\pm 1)^j \\ & \times \left(\frac{a_2}{R}\right)^j (j+1) P_{j0}(\cos(\alpha_2)) \\ & - P_{11}(\cos(\alpha_1))\cos(\beta_1 - \beta_2) \\ & \times \sum_{j=p+1}^{\infty} (\pm 1)^j \left(\frac{a_2}{R}\right)^j P_{j1}(\cos(\alpha_2)) \Bigg|, \\ c_1 = & \begin{cases} \frac{1}{2}, & p = 0 \\ 1, & p > 0. \end{cases} \end{aligned} \quad (55)$$

In our scheme we include all possible values of a_1. A box with coordinate ranges $[-1,\ldots,1,\ -1,\ldots,1,\ -1,\ldots,1]$ allows all values from 0 to $\sqrt{3}$. The angles α_1 and β_1 are treated differently. We include only the following 8 combinations of the angles $\alpha_1(0 \le \alpha_1 \le \pi)$ and $\beta_1(0 \le \beta_1 < 2\pi)$

$$(1)\ \cos(\alpha_{1,\ 1}) = +\frac{\sqrt{3}}{3},\ \cos(\beta_{1,\ 1}) = +\frac{\sqrt{2}}{2},\ \sin(\beta_{1,\ 1}) = +\frac{\sqrt{2}}{2},$$

$$(2)\ \cos(\alpha_{1,\ 2}) = +\frac{\sqrt{3}}{3},\ \cos(\beta_{1,\ 2}) = -\frac{\sqrt{2}}{2},\ \sin(\beta_{1,\ 2}) = +\frac{\sqrt{2}}{2},$$

$$(3)\ \cos(\alpha_{1,\ 3}) = +\frac{\sqrt{3}}{3},\ \cos(\beta_{1,\ 3}) = -\frac{\sqrt{2}}{2},\ \sin(\beta_{1,\ 3}) = -\frac{\sqrt{2}}{2},$$

$$(4)\ \cos(\alpha_{1,\ 4}) = +\frac{\sqrt{3}}{3},\ \cos(\beta_{1,\ 4}) = +\frac{\sqrt{2}}{2},\ \sin(\beta_{1,\ 4}) = -\frac{\sqrt{2}}{2},$$

$$(5)\ \cos(\alpha_{1,\ 5}) = -\frac{\sqrt{3}}{3},\ \cos(\beta_{1,\ 5}) = +\frac{\sqrt{2}}{2},\ \sin(\beta_{1,\ 5}) = +\frac{\sqrt{2}}{2},$$

$$(6)\ \cos(\alpha_{1,\ 6}) = -\frac{\sqrt{3}}{3},\ \cos(\beta_{1,\ 6}) = -\frac{\sqrt{2}}{2},\ \sin(\beta_{1,\ 6}) = +\frac{\sqrt{2}}{2},$$

$$(7)\ \cos(\alpha_{1,\ 7}) = -\frac{\sqrt{3}}{3},\ \cos(\beta_{1,\ 7}) = -\frac{\sqrt{2}}{2},\ \sin(\beta_{1,\ 7}) = -\frac{\sqrt{2}}{2},$$

$$(8)\ \cos(\alpha_{1,\ 8}) = -\frac{\sqrt{3}}{3},\ \cos(\beta_{1,\ 8}) = +\frac{\sqrt{2}}{2},\ \sin(\beta_{1,\ 8}) = -\frac{\sqrt{2}}{2}. \quad (56)$$

These eight combinations and $a_1(0 \le a_1 \le \sqrt{3})$ represent positions on the connecting lines from the box center to the eight corners of the box.

Now we compute the expression

$$\begin{aligned} \Bigg| & P_{10}(\cos(\alpha_1)) \sum_{j=p+1}^{\infty} (\pm 1)^j \left(\frac{a_2}{R}\right)^j (j+1) P_{j0}(\cos(\alpha_2)) \\ & - P_{11}(\cos(\alpha_1))\cos(\beta_1 - \beta_2) \sum_{j=p+1}^{\infty} (\pm 1)^j \left(\frac{a_2}{R}\right)^j P_{j1}(\cos(\alpha_2)) \Bigg| \end{aligned} \quad (57)$$

for each grid point $(a_2,\ \alpha_2,\ \beta_2)$. The term $(\pm 1)^j$ and the eight combinations of the angles α_1 and β_1 require 16 computations for each grid point. We compute the maximum of the 16 combinations and store the value as a function of the grid point $(a_2,\ \alpha_2,\ \beta_2)$ in a library. Similar to Eq. (54) we define the elements $F_{1p}(a_2,\ \alpha_2,\ \beta_2)$ as follows:

$$\begin{aligned} F_{1p}(a_2,\ \alpha_2,\ \beta_2) = \max_{n=1}^{8} \max_{s=-1,\ 1} \Bigg| & P_{10}(\cos(\alpha_{1,\ n})) \\ & \times \sum_{j=p+1}^{\infty} s^j \left(\frac{a_2}{R}\right)^j (j+1) P_{j0}(\cos(\alpha_2)) \\ & - P_{11}(\cos(\alpha_{1,\ n}))\cos(\beta_{1,\ n} - \beta_2) \\ & \times \sum_{j=p+1}^{\infty} s^j \left(\frac{a_2}{R}\right)^j P_{j1}(\cos(\alpha_2)) \Bigg|. \end{aligned} \quad (58)$$

The error term of the second order is given by

$$\Delta E_{l=2} = \frac{c_2}{R}\left(\frac{a_1}{R}\right)^2 \left| \frac{1}{2}P_{20}(\cos(\alpha_1)) \sum_{j=p+1}^{\infty} (\pm 1)^j \left(\frac{a_2}{R}\right)^j (j+1)(j+2)P_{j0}(\cos(\alpha_2)) - \frac{1}{3}P_{21}(\cos(\alpha_1))\cos(\beta_1-\beta_2) \sum_{j=p+1}^{\infty} (\pm 1)^j \right.$$
$$\left. \times \left(\frac{a_2}{R}\right)^j (j+2)P_{j1}(\cos(\alpha_2)) + \frac{1}{12}P_{22}(\cos(\alpha_1))\cos(2(\beta_1-\beta_2)) \sum_{j=p+1}^{\infty} (\pm 1)^j \left(\frac{a_2}{R}\right)^j P_{j2}(\cos(\alpha_2)) \right|, \quad c_2 = \begin{cases} 0, & p<1 \\ \frac{1}{2}, & p=1 \\ 1, & p>1. \end{cases} \tag{59}$$

Similar to Eqs. (54) and (58) we define the elements $F_{2p}(a_2,\ \alpha_2,\ \beta_2)$ as follows:

$$F_{2p}(a_2,\ \alpha_2,\ \beta_2) = \max_{n=1}^{8} \max_{s=-1,\ 1} \left| \frac{1}{2}P_{20}(\cos(\alpha_{1,\ n})) \sum_{j=p+1}^{\infty} s^j \left(\frac{a_2}{R}\right)^j (j+1)(j+2)P_{j0}(\cos(\alpha_2)) - \frac{1}{3}P_{21}(\cos(\alpha_{1,\ n}))\cos(\beta_{1,\ n}-\beta_2) \right.$$
$$\left. \times \sum_{j=p+1}^{\infty} s^j \left(\frac{a_2}{R}\right)^j (j+2)P_{j1}(\cos(\alpha_2)) + \frac{1}{12}P_{22}(\cos(\alpha_{1,\ n}))\cos(2(\beta_{1,\ n}-\beta_2)) \sum_{j=p+1}^{\infty} s^j \left(\frac{a_2}{R}\right)^j P_{j2}(\cos(\alpha_2)) \right|. \tag{60}$$

The error term of general order q is given by

$$\Delta E_{l=q} = \frac{c_q}{R}\left(\frac{a_1}{R}\right)^q \left| \frac{1}{q!}P_{q0}(\cos(\alpha_1)) \sum_{j=p+1}^{\infty} (\pm 1)^j \left(\frac{a_2}{R}\right)^j \frac{(j+q)!}{j!}P_{j0}(\cos(\alpha_2)) + 2\sum_{m=1}^{q} (-1)^m \frac{1}{(q+m)!}P_{qm}(\cos(\alpha_1))\cos(m(\beta_1-\beta_2)) \right.$$
$$\left. \times \sum_{j=p+1}^{\infty} (\pm 1)^j \left(\frac{a_2}{R}\right)^j \frac{(j+q)!}{(j+m)!}P_{jm}(\cos(\alpha_2)) \right|, \quad c_q = \begin{cases} 0, & p<q-1 \\ \frac{1}{2}, & p=q-1 \\ 1, & p>q-1, \end{cases} \quad q>1. \tag{61}$$

Similar to Eqs. (54), (58), and (60) we define the elements $F_{qp}(a_2,\ \alpha_2,\ \beta_2)$ as follows:

$$F_{qp}(a_2,\ \alpha_2,\ \beta_2) = \max_{n=1}^{8} \max_{s=-1,\ 1} \left| \frac{1}{q!}P_{q0}(\cos(\alpha_{1,\ n})) \sum_{j=p+1}^{\infty} s^j \left(\frac{a_2}{R}\right)^j \frac{(j+q)!}{j!}P_{j0}(\cos(\alpha_2)) + 2\sum_{m=1}^{q} (-1)^m \right.$$
$$\left. \times \frac{1}{(q+m)!}P_{qm}(\cos(\alpha_{1,\ n}))\cos(m(\beta_{1,\ n}-\beta_2)) \sum_{j=p+1}^{\infty} s^j \left(\frac{a_2}{R}\right)^j \frac{(j+q)!}{(j+m)!}P_{jm}(\cos(\alpha_2)) \right|, \quad q>0. \tag{62}$$

We take all the elements F_{qp} with $p \geq 0$ and $0 \leq q \leq p+1$ into account. To ensure symmetry we must use the Cartesian representation of F_{qp} with respect to the Cartesian axes X, Y, and Z. Assuming that each Cartesian coordinate ranges from -1 to 1 $[-1,\ldots,1,\ -1,\ldots,1,\ -1,\ldots,1]$ we introduce the elements H_{qp} as follows:

$$\begin{aligned} H_{qp}(x_2,\ y_2,\ z_2) = \max(&F_{qp}(s_x x_2,\ s_y y_2,\ s_z z_2), \\ &F_{qp}(s_x x_2,\ s_z z_2,\ s_y y_2), \\ &F_{qp}(s_y y_2,\ s_x x_2,\ s_z z_2), \\ &F_{qp}(s_y y_2,\ s_z z_2,\ s_x x_2), \\ &F_{qp}(s_z z_2,\ s_x x_2,\ s_y y_2), \\ &F_{qp}(s_z z_2,\ s_y y_2\ ,s_x x_2)), \end{aligned}$$

$$p \geq 0,\ \ 0 \leq q \leq p+1,$$

$$x_2 = -\frac{31}{32},\ -\frac{29}{32},\ldots,\ -\frac{1}{32},\ 0,\ \frac{1}{32},\ldots,\ \frac{29}{32},\ \frac{31}{32}, \tag{63}$$

$$y_2 = -\frac{31}{32},\ -\frac{29}{32},\ldots,\ -\frac{1}{32},\ 0,\ \frac{1}{32},\ldots,\ \frac{29}{32},\ \frac{31}{32},$$

$$z_2 = -\frac{31}{32},\ -\frac{29}{32},\ldots,\ -\frac{1}{32},\ 0,\ \frac{1}{32},\ldots,\ \frac{29}{32},\ \frac{31}{32},$$

$$s_x = \pm 1,\ \ s_y = \pm 1,\ \ s_z = \pm 1.$$

Due to symmetry we have to store only 969 grid points instead of 33^3 for each element H_{qp}. Equations (42) and (63) define a replacement system which has an energy error greater than or equal to the energy error of the original system. After we have derived the error terms of the second box we still have to include the neglected components of the first box. Because we did not apply a space domain decomposition in both boxes the only untreated coordinate is a_1, the distance of a particle in box A to the box center. Now we

include all particles of the first box, thus we change the notation of a_1 to a_I. We simply have to calculate the terms f_n given by

$$f_n^{\text{box A}} = \sum_{I=1}^{N^{\text{box A}}} |q_I| \left(\frac{a_I}{R}\right)^n. \tag{64}$$

In Eq. (64) q_I is a particle charge. We compute the sum in Eq. (64) for $n=0,\ 4,\ 9,\ 18,\ 36,\ 45$ for each box on each level of the FMM tree using a look-up table to minimize the computational effort. For two separated boxes we treat all possible $ws+1$ displacements $(s=1,\ldots,ws+1)$ of the two box centers in 1D [Eq. (42)] separately. Now we can modify Eq. (64) slightly

$$f_{ns}^{\text{box A}} = \left(\frac{R_1}{R_s}\right)^n \sum_{I=1}^{N^{\text{box A}}} |q_I| \left(\frac{a_I}{R_1}\right)^n, \quad 0 \le a_I \le \frac{\sqrt{3}}{2^L},$$

$$R_s = \frac{ws+s}{2^{L-1}}, \quad s=1,\ldots,ws+1, \tag{65}$$

$$0 \le \left(\frac{a_I}{R_1}\right) \le \frac{\sqrt{3}}{2(ws+1)}.$$

The elements $f_{ns}^{\text{box A}}$ allow to compute the global error terms Q_{nsL}

$$Q_{nsL}(G) = 2 \sum_{B(L)} \max_{A(s,B)} \tilde{Q}_G^{\text{box B}} f_{ns}^{\text{box A}}, \quad s=1,\ldots,ws+1,$$
$$n=0,\ 4,\ 9,\ 18,\ 36,\ 45 \tag{66}$$

with

$$\tilde{Q}_G^{\text{box B}} = \sum_{J_B(G)} |q_{J_B}|. \tag{67}$$

The term q_{J_B} represents a charge in the corresponding grid box. The interaction list $A(s,\ B)$ in Eq. (66) covers all boxes which have a far field interaction with box B separated by R_s in 1D. The neglected term [Eq. (51)] is taken into account by the summation over B in Eq. (66) when we combine the Q_{nsL} with the grid contribution of box B. Because we take the maximum and do not sum up in Eq. (66) we have to multiply by a factor of 2 to maintain the symmetry with respect to the error contribution, since the symmetry condition $B=C_m$ with

$$A_m = \max_{A(s,B)} f_{ns}^{\text{box A}} \tag{68}$$

and

$$C_m = \max_{C(s,A_m)} f_{ns}^{\text{box C}} \tag{69}$$

is usually not satisfied.

Because we compute the terms Q_{nsL} only for $n=0,\ 4,\ 9,\ 18,\ 36,\ 45$ we use an interpolation scheme to obtain the missing values. In case the box contains two or more particles or the particle is not located in the box center the following relations:

$$Q_{0,\ sL} > Q_{4,\ sL} > Q_{9,\ sL} > Q_{18,\ sL} > Q_{36,\ sL} > Q_{45,\ sL} > 0 \tag{70}$$

are satisfied. This scheme has to ensure the correct asymptotic behavior for infinite n. The complete set of the elements Q_{nsL} is given by

$$Q_{nsL} = \begin{cases} Q_{0,\ 4;\ sL}, & 0 \le n < 4 \\ Q_{4,\ 9;\ sL}, & 4 \le n < 9 \\ Q_{9,\ 18;\ sL}, & 9 \le n < 18 \\ Q_{18,\ 36;\ sL}, & 18 \le n < 36 \\ Q_{36,\ 45;\ sL}, & 36 \le n < \infty. \end{cases} \tag{71}$$

The interpolation scheme can be described as follows. We start with the term $Q_{36,\ 45;\ sL}$ using the terms $Q_{36,\ sL}$ and $Q_{45,\ sL}$ and an exponential interpolation ansatz. $Q_{36,\ 45;\ sL}$ is now given by

$$Q_{36,\ 45;\ sL} = \frac{Q_{36,\ sL}^5}{Q_{45,\ sL}^4} \left(\sqrt[9]{\frac{Q_{45,\ sL}}{Q_{36,\ sL}}}\right)^n. \tag{72}$$

All the remaining terms in Eq. (71) can now easily be determined. Again, we use an exponential interpolation ansatz to determine the term $Q_{18,\ 36;\ sL}$

$$Q_{18,\ 36;\ sL} = e^{A_{18,\ 36;\ sL} n^2 + B_{18,\ 36;\ sL} n + C_{18,\ 36;\ sL}}. \tag{73}$$

The coefficients $A_{18,\ 36;\ sL}$, $B_{18,\ 36;\ sL}$, and $C_{18,\ 36;\ sL}$ can be obtained from the following system of equations:

$$Q_{18,\ 36;\ sL}(18) = Q_{18,\ sL}$$
$$Q_{18,\ 36;\ sL}(36) = Q_{36,\ sL} \tag{74}$$
$$\frac{dQ_{18,\ 36;\ sL}(36)}{dn} = \frac{dQ_{36,\ 45;\ sL}(36)}{dn}.$$

The first derivative of $Q_{18,\ 36;\ sL}$ must be less than 0 and the curvature

$$\frac{\dfrac{d^2 Q_{18,\ 36;\ sL}}{dn^2}}{\sqrt{1 + \left(\dfrac{dQ_{18,\ 36;\ sL}}{dn}\right)^2}^3} \tag{75}$$

greater than 0 for $18 \le n \le 36$. In case the coefficients $A_{18,\ 36;\ sL}$, $B_{18,\ 36;\ sL}$, and $C_{18,\ 36;\ sL}$ do not satisfy the two conditions

$$\frac{dQ_{18,\ 36;\ sL}}{dn} < 0, \quad \frac{d^2 Q_{18,\ 36;\ sL}}{dn^2} > 0, \quad 18 \le n \le 36 \tag{76}$$

which are identical to

$$2A_{18,\ 36;\ sL}n + B_{18,\ 36;\ sL} < 0,$$
$$(2A_{18,\ 36;\ sL}n + B_{18,\ 36;\ sL})^2 + 2A_{18,\ 36;\ sL} > 0, \quad 18 \le n \le 36 \tag{77}$$

and in case $A_{18,\ 36;\ sL} < 0$

$$B_{18,\ 36;\ sL} < 2|A_{18,\ 36;\ sL}|n,$$
$$|2A_{18,\ 36;\ sL}n + B_{18,\ 36;\ sL}| > \sqrt{2|A_{18,\ 36;\ sL}|}, \tag{78}$$
$$A_{18,\ 36;\ sL} < 0, \quad 18 \le n \le 36$$

we ignore the demand for differentiability. The coefficients are now given by the following system of equations:

$$A_{18,\ 36;\ sL} = 0$$
$$Q_{18,\ 36;\ sL}(18) = Q_{18,\ sL} \tag{79}$$
$$Q_{18,\ 36;\ sL}(36) = Q_{36,\ sL}.$$

The terms $Q_{9,\ 18;\ sL}$, $Q_{4,\ 9;\ sL}$, and $Q_{0,\ 4;\ sL}$ are determined similarly in the given order. The elements Q_{nsL} [Eq. (71)] are strictly monotonic decreasing with respect to n. It should be noted, that our interpolation scheme provides a sufficient accuracy to our FMM error estimation scheme.

Finally we obtain a relation between the level of poles p and a user-requested absolute energy threshold ΔE_{req} $(\Delta E_{\text{req}} > 0)$

$$\Delta E_{\text{req}} \ge \sum_L \sum_G \max_{s=1}^{ws+1} \frac{1}{R_s}\left(\frac{ws+1}{ws+s}\right)^{p+1} \max\Big(Q_{0sL}(G)H_{0p}(G) + cQ_{1sL}(G)H_{1p}(G),$$
$$Q_{0sL}(G)H_{0p}(G), \ldots, Q_{psL}(G)H_{pp}(G), \ \frac{1}{2}Q_{p+1,\ sL}(G)H_{p+1,\ p}(G)\Big), \ c = \begin{cases} \frac{1}{2}, & p = 0 \\ 1, & p > 0 \end{cases} \tag{80}$$

with

$$R_s = \frac{ws+s}{2^{L-1}}. \tag{81}$$

Because of the factor 1/2 in front of the second triple sum in Eq. (50) we have to multiply the product $Q_{p+1,\ sL}(G)H_{p+1,\ p}(G)$ by 1/2. All terms $H_{0,\ldots,p+1,\ p}$ contain the common factor $R^{-(p+1)}$ which is leading to the term $((ws+1)/(ws+s))^{p+1}$ in Eq. (80). Now we are able to obtain the final relation to determine p

$$\Delta E_{\text{req}} \ge \sum_L \sum_G \max_{s=1}^{ws+1} \frac{2^{L-1}}{ws+1}\left(\frac{ws+1}{ws+s}\right)^{p+2} \max\Big(Q_{0sL}(G)H_{0p}(G) + cQ_{1sL}(G)H_{1p}(G),$$
$$Q_{0sL}(G)H_{0p}(G), \ldots, Q_{psL}(G)H_{pp}(G), \ \frac{1}{2}Q_{p+1,\ sL}(G)H_{p+1,\ p}(G)\Big), \ c = \begin{cases} \frac{1}{2}, & p = 0 \\ 1, & p > 0. \end{cases} \tag{82}$$

In case far field contributions of the energy have to be taken into account [Eq. (38)] we obtain the minimal level of poles when we start at $p=0$ and increment p until the right hand side of Eq. (82) is less than or equal to ΔE_{req}.

In addition we can also compute an approximation of the error ΔE for $p=0$ by a power series expansion of the particle positions with respect to the box centers. Assuming $\mathbf{R}_K=(x_K,y_K,z_K)^T$ and $\mathbf{R}_M=(x_M,y_M,z_M)^T$ are the coordinates of the centers of box K and box M, respectively, we can write

$$E = \frac{1}{2}\sum_L \sum_{K(L)} \sum_{M(K)} \sum_{k=1}^{N_K} \sum_{m=1}^{N_M} \frac{q_k q_m}{\sqrt{(x_k-x_m)^2 + (y_k-y_m)^2 + (z_k-z_m)^2}}. \tag{83}$$

The upper bounds N_K and N_M indicate the number of particles in the boxes. The energy error can be written as follows

$$\Delta E_{p=0} = \frac{1}{2}\sum_L \sum_{I(L)} \sum_{J(I)} \Bigg(\left| \sum_{i=1}^{N_I} \frac{\partial E}{\partial x_i}(\mathbf{R}_I, \mathbf{R}_J)(x_i - x_I) \right| + \left| \sum_{i=1}^{N_I} \frac{\partial E}{\partial y_i}(\mathbf{R}_I, \mathbf{R}_J)(y_i - y_I) \right| + \left| \sum_{i=1}^{N_I} \frac{\partial E}{\partial z_i}(\mathbf{R}_I, \mathbf{R}_J)(z_i - z_I) \right|$$
$$+ \left| \sum_{j=1}^{N_J} \frac{\partial E}{\partial x_j}(\mathbf{R}_I, \mathbf{R}_J)(x_j - x_J) \right| + \left| \sum_{j=1}^{N_J} \frac{\partial E}{\partial y_j}(\mathbf{R}_I, \mathbf{R}_J)(y_j - y_J) \right| + \left| \sum_{j=1}^{N_J} \frac{\partial E}{\partial z_j}(\mathbf{R}_I, \mathbf{R}_J)(z_j - z_J) \right|$$
$$+ \left| \sum_{i=1}^{N_I} \sum_{j=1}^{N_J} \frac{\partial^2 E(\mathbf{R}_I, \mathbf{R}_J)}{\partial x_i \partial x_j}(x_i - x_I)(x_j - x_J) \right| + \left| \sum_{i=1}^{N_I} \sum_{j=1}^{N_J} \frac{\partial^2 E(\mathbf{R}_I, \mathbf{R}_J)}{\partial x_i \partial y_j}(x_i - x_I)(y_j - y_J) \right|$$

$$+\left|\sum_{i=1}^{N_I}\sum_{j=1}^{N_J}\frac{\partial^2 E(\mathbf{R}_I,\ \mathbf{R}_J)}{\partial x_i\,\partial z_j}(x_i-x_I)(z_j-z_J)\right|+\left|\sum_{i=1}^{N_I}\sum_{j=1}^{N_J}\frac{\partial^2 E(\mathbf{R}_I,\ \mathbf{R}_J)}{\partial y_i\,\partial x_j}(y_i-y_I)(x_j-x_J)\right|$$
$$+\left|\sum_{i=1}^{N_I}\sum_{j=1}^{N_J}\frac{\partial^2 E(\mathbf{R}_I,\ \mathbf{R}_J)}{\partial y_i\,\partial y_j}(y_i-y_I)(y_j-y_J)\right|+\left|\sum_{i=1}^{N_I}\sum_{j=1}^{N_J}\frac{\partial^2 E(\mathbf{R}_I,\ \mathbf{R}_J)}{\partial y_i\,\partial z_j}(y_i-y_I)(z_j-z_J)\right|$$
$$+\left|\sum_{i=1}^{N_I}\sum_{j=1}^{N_J}\frac{\partial^2 E(\mathbf{R}_I,\ \mathbf{R}_J)}{\partial z_i\,\partial x_j}(z_i-z_I)(x_j-x_J)\right|+\left|\sum_{i=1}^{N_I}\sum_{j=1}^{N_J}\frac{\partial^2 E(\mathbf{R}_I,\ \mathbf{R}_J)}{\partial z_i\,\partial y_j}(z_i-z_I)(y_j-y_J)\right|$$
$$+\left|\sum_{i=1}^{N_I}\sum_{j=1}^{N_J}\frac{\partial^2 E(\mathbf{R}_I,\ \mathbf{R}_J)}{\partial z_i\,\partial z_j}(z_i-z_I)(z_j-z_J)\right|\Bigg). \tag{84}$$

If we neglect the absolute value of each term in Eq. (84) and compute the right hand side of Eq. (84) we obtain the far field energy for $p=1$, $E_{p=1}$ minus the far field energy for $p=0$, $E_{p=0}$

$$E_{p=1}-E_{p=0}=\frac{1}{2}\sum_L\sum_{I(L)}\sum_{J(I)}\sum_{l=0}^{1}\sum_{m=-l}^{l}\sum_{j=0}^{1}\sum_{k=-j}^{j}(-1)^j \times\omega_{lm}(\mathbf{R}_I)B_{j+l,\ k+m}\omega_{jk}(\mathbf{R}_J) -\frac{1}{2}\sum_L\sum_{I(L)}\sum_{J(I)}\omega_{00}(\mathbf{R}_I)\frac{1}{|\mathbf{R}_I-\mathbf{R}_J|}\omega_{00}(\mathbf{R}_J) \tag{85}$$

with

$$\omega_{00}=\sum_{k=1}^{N_K}q_k, \tag{86}$$

$$\omega_{10}=\sum_{k=1}^{N_K}q_k(z_k-z_K), \tag{87}$$

$$\omega_{11}=\frac{1}{2}\sum_{k=1}^{N_K}q_k((x_k-x_K)-i(y_k-y_K)), \tag{88}$$

and

$$\omega_{1,-1}=-\frac{1}{2}\sum_{k=1}^{N_K}q_k((x_k-x_K)+i(y_k-y_K)). \tag{89}$$

The terms $B_{j+l,\ k+m}$ represent the elements of the operator $\mathbf{B}$.[4,5] In Eq. (84) we sum over all levels and all box-box interactions and neglect all contributions of higher order. The partial derivatives in Eq. (84) depend only on particle charges and the differences x_I-x_J, y_I-y_J, and z_I-z_J. The Cartesian coordinates x_I, y_I, and z_I as well as x_J, y_J, and z_J are the coordinates of the box centers. We have to compute the terms

$$\left|\sum_{k=1}^{N_K}q_k\right|,\quad\left|\sum_{k=1}^{N_K}q_k(x_k-x_K)\right|,\quad\left|\sum_{k=1}^{N_K}q_k(y_k-y_K)\right|,\quad\left|\sum_{k=1}^{N_K}q_k(z_k-z_K)\right| \tag{90}$$

for all boxes on all levels of the FMM tree in order to compute $\Delta E_{p=0}$ [Eq. (84)]. Usually $\Delta E_{p=0}$ is not very different from the right hand side of Eq. (82) for $p=0$. Now we can use the relation

$$\Delta E_{\mathrm{req}}\geq\max\left(\sum_L\sum_G\max_{s=1}^{ws+1}\frac{2^{L-1}}{ws+1}\left(\frac{ws+1}{ws+s}\right)^2\left(Q_{0sL}(G)H_{00}(G)+\frac{1}{2}Q_{1sL}(G)H_{10}(G)\right),\ \Delta E_{p=0}\right) \tag{91}$$

in addition to Eq. (82) to improve the FMM error estimation scheme for $p=0$. We can combine Eqs. (82) and (91) using the Kronecker delta δ_{0p}

$$\Delta E_{\mathrm{req}}\geq\max\left(\sum_L\sum_G\max_{s=1}^{ws+1}\frac{2^{L-1}}{ws+1}\left(\frac{ws+1}{ws+s}\right)^{p+2}\max\left(Q_{0sL}(G)H_{0p}(G)+cQ_{1sL}(G)H_{1p}(G),\right.\right.$$
$$\left.\left.Q_{0sL}(G)H_{0p}(G),\ldots,Q_{psL}(G)H_{pp}(G),\ \frac{1}{2}Q_{p+1,\ sL}(G)H_{p+1,\ p}(G)\right),\ \delta_{0p}\Delta E_{p=0}\right),\quad c=\begin{cases}\frac{1}{2}, & p=0\\ 1, & p>0.\end{cases} \tag{92}$$

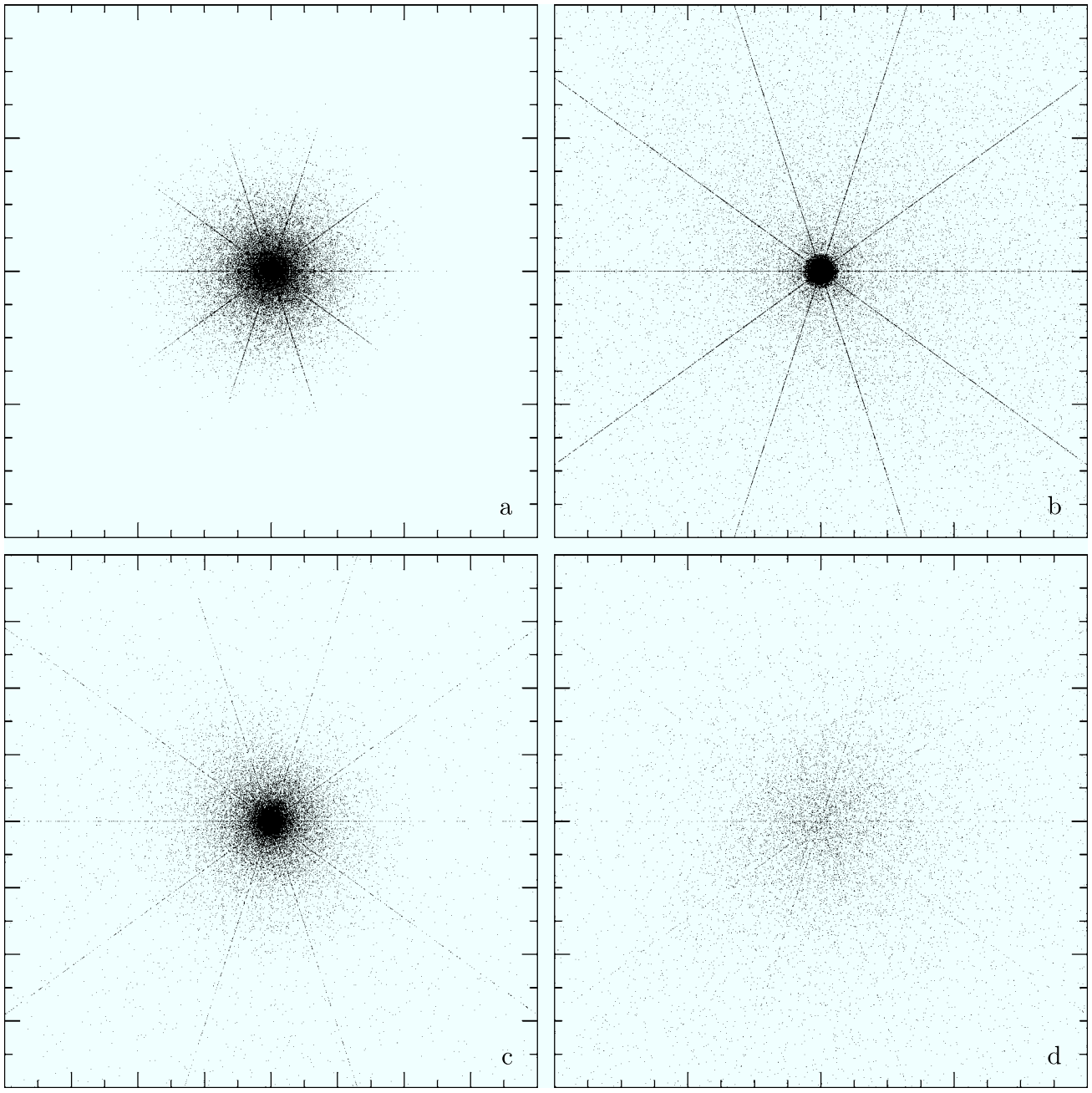

FIG. 6. 2D representation of a particle system as a result of a laser-induced Coulomb explosion. The two axes range (a) from 0 to 1, all 114 537 particles in 100% of the volume, (b) from 0.4375 to 0.5625, 78 946 particles (68.9% of all particles) in 1/512 of the volume, (c) from 0.492 187 5 to 0.507 812 5, 41 684 particles (36.4% of all particles) in 1/262 144 of the volume, and (d) from 0.499 023 437 5 to 0.500 976 562 5, 21 892 particles (19.1% of all particles) in 1/134 217 728 of the volume of the simulation box are shown.

III. RESULTS

We have verified the correctness of our FMM error estimation scheme by many test calculations. Homogeneous as well as inhomogeneous distributions have been tested. Table III shows the results for a particle system consisting of 100 000 particles each with charge 1 distributed along the Z axis which represents a system of inhomogeneously distributed particles in 3D. Table IV shows the results for a clustered particle system which is a result of a laser-induced Coulomb explosion[12–16] (Fig. 6). This figure shows the same particle distribution with different zoom levels to visualize the strong clustering. We have performed all reference calculations in quadruple precision (128 bits for the representation of a floating point number) to exclude any numerical errors. In the ANSI/IEEE standard the relative error of the binary representation of floating point numbers in double precision is $2^{-52} \approx 2.220 \times 10^{-16}$. However, the absolute energy error of 0.0171×10^{-7} in Table IV is equivalent to a relative energy error of 8.615×10^{-17} which is less than 2^{-52}. In addition we had to ensure an exact computation of the near field contributions which is possible only in quadruple precision for relative errors in the range of 2^{-52}. The FMM errors do not exceed the user-requested energy thresholds. The results shown in Tables III and IV prove the correctness of our approach. Table V shows the comparison of our FMM error estimation scheme with two other approaches for the

TABLE III. Comparison of user-requested absolute energy errors with the absolute energy errors of FMM calculations for a system consisting of 100 000 particles each with charge 1 distributed along the Z axis $(x_i=0,\ y_i=0,\ z_i=i,\ i=1,\ldots,100\,000)$. $E_{\text{exact}}=1\,109\,014.612\,986\,342\,794\,736$.

Requested error	Level of poles	FMM energy error
10^{+6}	0	$0.0384\times10^{+6}$
10^{+5}	2	$0.1237\times10^{+5}$
10^{+4}	5	$0.0785\times10^{+4}$
10^{+3}	8	$0.0039\times10^{+3}$
10^{+2}	12	$0.0385\times10^{+2}$
10^{+1}	17	$0.0311\times10^{+1}$
10^{+0}	22	$0.0390\times10^{+0}$
10^{-1}	27	0.0494×10^{-1}
10^{-2}	32	0.0767×10^{-2}
10^{-3}	38	0.0435×10^{-3}
10^{-4}	44	0.0180×10^{-4}
10^{-5}	50	0.0444×10^{-5}

FMM separation criterion $ws=1$. The last two columns of Table V show the solutions of the following two equations proposed by White and Head-Gordon[4]

$$\Delta E_{\text{req}}^{\text{truncation}} \geq \frac{1}{2}\sum_{L}\sum_{K(L)}\sum_{M(K)} \frac{\left(\Sigma_{I=1}^{N^{\text{box}\ K}}|q_I|\right)\left(\Sigma_{J=1}^{N^{\text{box}\ M}}|q_J|\right)}{(3-\sqrt{3})2^{-L}}\left(\frac{\sqrt{3}}{3}\right)^{p+1} \tag{93}$$

and

$$\Delta E_{\text{req}}^{\text{operator}\ \mathbf{B}} \geq \frac{1}{2}\sum_{L}\sum_{K(L)}\sum_{M(K)} \frac{\left(\Sigma_{I=1}^{N^{\text{box}\ K}}|q_I|\right)\left(\Sigma_{J=1}^{N^{\text{box}\ M}}|q_J|\right)}{(4-2\sqrt{3})2^{-L}}\left(\frac{\sqrt{3}}{2}\right)^{p+1}. \tag{94}$$

Equation (93) may overestimate and underestimate the level of poles depending on the user-requested energy threshold. Table V and Fig. 7 show a crossover point at a user-requested absolute energy threshold of 10^{-3} with respect to the level of poles. For higher levels of poles the error due to the use of operator **B** is dominant. Equation (94) always highly overestimates the level of poles. Therefore this error estimation is without any practical relevance. Table VI shows the ratio of the computational effort in the multipole-to-local translations resulting from our FMM error estimation scheme and the error estimator which includes the error from the truncation of the expansions but ignores the error as a consequence of the use of operator **B**. To compare our FMM error estimation approach against Chebyshev based schemes

TABLE IV. Comparison of user-requested absolute energy errors with the absolute energy errors of FMM calculations for a system consisting of 114 537 inhomogeneously distributed positive charges. $E_{\text{exact}}=19\,812\,647.020\,360\,131\,248\,825$.

Requested error	Level of poles	FMM energy error
10^{+7}	0	$0.1163\times10^{+7}$
10^{+6}	1	$0.0512\times10^{+6}$
10^{+5}	3	$0.0681\times10^{+5}$
10^{+4}	5	$0.0185\times10^{+4}$
10^{+3}	7	$0.0020\times10^{+3}$
10^{+2}	8	$0.0251\times10^{+2}$
10^{+1}	10	$0.0213\times10^{+1}$
10^{+0}	14	$0.0169\times10^{+0}$
10^{-1}	18	0.0089×10^{-1}
10^{-2}	22	0.0145×10^{-2}
10^{-3}	27	0.0130×10^{-3}
10^{-4}	32	0.0064×10^{-4}
10^{-5}	37	0.0195×10^{-5}
10^{-6}	42	0.0098×10^{-6}
10^{-7}	48	0.0171×10^{-7}

TABLE V. Levels of poles for three different error estimators depending on user-requested absolute energy errors for a system consisting of 100 000 particles each with charge 1 distributed along the Z axis $(x_i=0,\ y_i=0,\ z_i=i,\ i=1,\ldots,100\,000)$. The second column shows the levels of poles as a result of our FMM error estimation scheme. The next two columns show the levels of poles due to the truncation of the expansions and the use of operator **B**, respectively, (Ref. 4). The FMM separation criterion ws is equal to 1.

Requested error	FMM error estimation scheme	Truncation of expansions	Operator **B**
10^{+6}	0	1	11
10^{+5}	2	5	26
10^{+4}	5	9	41
10^{+3}	8	13	57
10^{+2}	12	18	72
10^{+1}	17	22	88
10^{+0}	22	26	103
10^{-1}	27	30	119
10^{-2}	32	34	135
10^{-3}	38	38	151
10^{-4}	44	42	165
10^{-5}	50	46	181

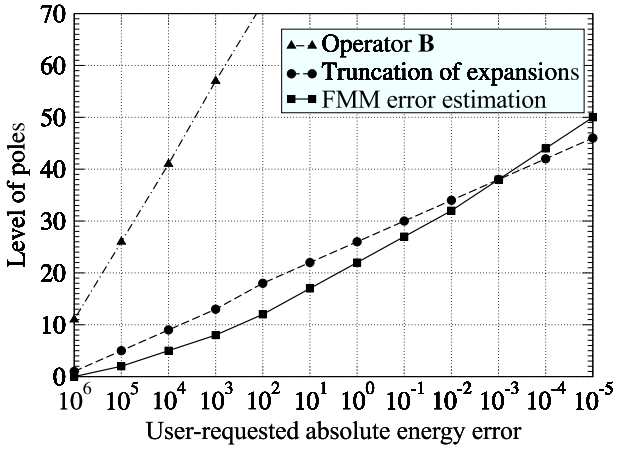

FIG. 7. Levels of poles for three different error estimators depending on user-requested absolute energy errors for a system consisting of 100 000 particles each with charge 1 distributed along the Z axis $(x_i=0,\ y_i=0,\ z_i=i,\ i=1,\ldots,100\,000)$. The solid line shows the level of poles as a result of our FMM error estimation scheme. The dashed and dot-dashed lines show the level of poles due to the truncation of the expansions and the use of operator **B**, respectively (Ref. 4). The FMM separation criterion ws is equal to 1. The solid and dashed line show a crossover point at a user-requested absolute energy error of 10^{-3}.

TABLE VI. Levels of poles for two different error estimators depending on user-requested relative energy errors and the resulting ratios of the number of floating point operations in the multipole-to-local translations of the rotation based FMM for 8^7 homogeneously distributed particles each with charge 1. The Cartesian coordinates are given by $x_i=2^{-7}i-2^{-8}$, $y_j=2^{-7}j-2^{-8}$, $z_k=2^{-7}k-2^{-8}$, $i, j, k=1,\ldots,2^7$.

Requested error	FMM error estimation scheme	Truncation of expansions	Ratio
10^{-01}	0	6	863.0
10^{-02}	1	11	156.9
10^{-03}	3	15	50.8
10^{-04}	5	19	31.4
10^{-05}	7	23	23.8
10^{-06}	9	27	19.8
10^{-07}	12	32	15.1
10^{-08}	15	36	11.6
10^{-09}	19	40	8.2
10^{-10}	22	44	7.2
10^{-11}	27	48	5.2
10^{-12}	31	52	4.4
10^{-13}	36	57	3.8
10^{-14}	41	61	3.2
10^{-15}	47	65	2.6

we will use Eq. (93) to formulate a Chebyshev based FMM. We substitute the infinite sum

$$\sum_{l=0}^{\infty} P_l(\cos(\gamma))\left(\frac{\sqrt{3}}{3}\right)^l \tag{95}$$

by a continuous Chebyshev expansion

$$\sum_{l=0}^{\infty} P_l(\cos(\gamma))\left(\frac{\sqrt{3}}{3}\right)^l = \sum_{n=0}^{\infty} c_n T_n(\cos(\gamma)) \tag{96}$$

with

$$c_n = \frac{2}{(1+\delta_{0n})\pi}\sum_{m=0}^{\infty}\left(\frac{\sqrt{3}}{3}\right)^m \int_0^{\pi} P_m(\cos(\chi))T_n(\cos(\chi))d\chi. \tag{97}$$

The terms T_n are the Chebyshev polynomials of the first kind with the property

TABLE VII. The first coefficients of the continuous Chebyshev expansion.

n	c_n
0	$1.103\,845\,772\,797\,212\,254\,324\,837\,694\,207\,631\,41\times10^{+0}$
1	$6.695\,374\,010\,430\,205\,408\,788\,168\,498\,427\,249\,92\times10^{-1}$
2	$2.949\,230\,814\,010\,860\,474\,878\,727\,980\,796\,395\,52\times10^{-1}$
3	$1.431\,541\,047\,730\,706\,872\,850\,138\,697\,133\,513\,40\times10^{-1}$
4	$7.271\,229\,360\,379\,197\,232\,089\,297\,595\,186\,401\,43\times10^{-2}$
5	$3.792\,178\,441\,399\,177\,265\,686\,781\,031\,292\,715\,29\times10^{-2}$
6	$2.012\,322\,319\,533\,058\,507\,666\,497\,404\,019\,992\,53\times10^{-2}$
7	$1.081\,011\,470\,983\,601\,176\,693\,107\,630\,403\,385\,75\times10^{-2}$
8	$5.860\,437\,744\,773\,163\,461\,910\,887\,476\,344\,235\,66\times10^{-3}$
9	$3.199\,641\,127\,137\,935\,053\,370\,857\,369\,821\,271\,15\times10^{-3}$
10	$1.756\,796\,962\,916\,457\,779\,346\,996\,992\,861\,958\,00\times10^{-3}$

TABLE VIII. Levels of poles for two different error estimators depending on user-requested relative energy errors and the resulting ratios of the number of floating point operations in the multipole-to-local translations of the rotation based FMM for 8^7 homogeneously distributed particles each with charge 1. The standard error estimation is improved by Chebyshev economization. The Cartesian coordinates are given by $x_i=2^{-7}i-2^{-8}$, $y_j=2^{-7}j-2^{-8}$, $z_k=2^{-7}k-2^{-8}$, $i, j, k=1,\ldots,2^7$.

Requested error	FMM error estimation scheme	Chebyshev economization	Ratio
10^{-01}	0	5	559.5
10^{-02}	1	9	93.1
10^{-03}	3	13	34.5
10^{-04}	5	17	23.1
10^{-05}	7	21	18.4
10^{-06}	9	25	15.9
10^{-07}	12	29	11.4
10^{-08}	15	33	9.1
10^{-09}	19	37	6.6
10^{-10}	22	41	5.9
10^{-11}	27	45	4.3
10^{-12}	31	49	3.7
10^{-13}	36	54	3.2
10^{-14}	41	58	2.7
10^{-15}	47	62	2.2

$$\int_0^{\pi} T_m(\cos(\chi))T_n(\cos(\chi))d\chi = (1+\delta_{0m})\frac{\pi}{2}\delta_{mn}. \tag{98}$$

The first coefficients of the continuous Chebyshev expansion are shown in Table VII. Equation (93) can now be improved

$$\Delta E_{\text{req}}^{\text{Chebyshev}} \geq \frac{1}{2}\sum_{L}\sum_{K(L)}\sum_{M(K)}\frac{\left(\Sigma_{I=1}^{N^{\text{box}\ K}}|q_I|\right)\left(\Sigma_{J=1}^{N^{\text{box}\ M}}|q_J|\right)}{3\times 2^{-L}} \times \sum_{n=p+1}^{\infty}|c_n|. \tag{99}$$

Table VIII shows the result of the Chebyshev economization. The improvement in comparison to Eq. (93) is marginal. Depending on the user-requested relative energy error the levels of poles are certainly smaller but not much. Even in case Chebyshev economization is used our FMM error estimation scheme is still much more efficient (Table VIII). The levels of poles determined by the first and second stage of our FMM error estimation scheme should be approximately the same for systems consisting of homogeneously distributed particles with uniform charge. Table IX shows that for a range of user-requested relative energy errors the levels of poles satisfy this condition. The overall behavior of our FMM error estimation scheme is also $\mathcal{O}(N)$ with respect to the number of particles N (Table X) because the prefactor of the $\mathcal{O}(N\log N)$ scaling part, the computation of the terms $f_n^{\text{box}\ A}$ [Eq. (64)] on each level of the FMM tree is very small and seems to be negligible. The Tables XI and XII show that operator **C** does not have any impact on the FMM results. Table XI shows the errors of two FMM calculations, one with use of the operator **C** and the second one without for single [floating point numbers (FPN) in 32 bits representation], double (FPN in 64 bits representation), and quadruple

TABLE IX. Comparison of the levels of poles determined by the first and second stage of the FMM error estimation scheme for 8^7 homogeneously distributed particles each with charge 1. The requested errors are user-requested relative energy errors. The Cartesian coordinates are given by $x_i=2^{-7}i-2^{-8}$, $y_j=2^{-7}j-2^{-8}$, $z_k=2^{-7}k-2^{-8}$, $i, j, k=1,\ldots,2^7$.

Requested error	Level of poles (first stage)	Level of poles (second stage)
10^{-01}	0	0
10^{-02}	2	1
10^{-03}	3	3
10^{-04}	5	5
10^{-05}	7	7
10^{-06}	10	9
10^{-07}	12	12
10^{-08}	15	15
10^{-09}	19	19
10^{-10}	23	22
10^{-11}	27	27
10^{-12}	32	31
10^{-13}	37	36
10^{-14}	42	41
10^{-15}	48	47

precision (FPN in 128 bits representation). We have compared four results, the energy computed by the product of multipole moments and Taylor coefficients

$$E_1=\frac{1}{2}\sum_{L}\sum_{I(L)}\sum_{l=0}^{p}\sum_{m=-l}^{l}\omega_{lm}^{\text{box I}}\mu_{lm}^{\text{box I}},$$
$$E_1^{\mathbf{C}}=\frac{1}{2}\sum_{I(\text{Depth}+1)}\sum_{l=0}^{p}\sum_{m=-l}^{l}\omega_{lm}^{\mathbf{C},\ \text{box I}}\mu_{lm}^{\mathbf{C},\ \text{box I}}, \tag{100}$$

the energy computed from the potential

$$E_2=\frac{1}{2}\sum_{i=1}^{N}q_i\Phi_i,$$
$$E_2^{\mathbf{C}}=\frac{1}{2}\sum_{i=1}^{N}q_i\Phi_i^{\mathbf{C}}, \tag{101}$$

and finally the components of the potential and gradient. Now we can define the following relative errors

TABLE X. Scaling of the two stages of the FMM error estimation scheme with respect to the number of particles N for homogeneously distributed particles each with charge 1. The numbers in columns 2–4 show the increase in the number of floating point operations with respect to the eight times smaller particle system. The scaling is $\mathcal{O}(N)$.

Number of particles	First stage	Second stage	First and second stage
8^6	9.501	9.574	9.565
8^7	9.058	8.942	8.956
8^8	8.814	8.642	8.663
8^9	8.678	8.509	8.530
8^{10}	8.596	8.435	8.456

$$\Delta_1=\frac{|E_1-E_1^{\mathbf{C}}|}{\min(|E_1|,\ |E_1^{\mathbf{C}}|)}, \tag{102}$$

$$\Delta_2=\frac{|E_2-E_2^{\mathbf{C}}|}{\min(|E_2|,\ |E_2^{\mathbf{C}}|)}, \tag{103}$$

$$\Delta_3=\max_{i=1}^{N}\left(\frac{|\Phi_i-\Phi_i^{\mathbf{C}}|}{\min(|\Phi_i|,\ |\Phi_i^{\mathbf{C}}|)}\right), \tag{104}$$

and

$$\Delta_4=\max_{i=1}^{N}\left(\frac{|\nabla_i-\nabla_i^{\mathbf{C}}|}{\min(|\nabla_i|,\ |\nabla_i^{\mathbf{C}}|)}\right). \tag{105}$$

We have done the calculations on the particle system shown in Table IV and in Fig. 6 for a user-requested absolute energy error of $\Delta E_{\text{req}}=10$ ($N=114537$, $p=10$, Depth=7). The energies and all components of the potential and gradient are nonzero. Table XII shows that Δ_1, Δ_2, Δ_3, and Δ_4 completely utilize the precision increase of the binary floating point representation by changing from double to quadruple precision.

IV. SUMMARY

We have presented a two-stage error estimation scheme. It incorporates the error contribution of each particle to the FMM error and can be applied to homogeneous as well as inhomogeneous particle systems. The FMM error is correlated with a user-requested threshold. In our current FMM implementation this threshold is either the absolute or relative energy error. In the first stage of our error estimation scheme homogeneous distributions in all boxes on all tree levels are assumed. In case a relative energy error is specified we have to compute an approximation of the energy to obtain the absolute energy error used in the error estimation scheme. The far field energy is approximated by the monopole energy. Additionally we have developed an approach to estimate the energy contribution of the interaction of charges in a single box as accurate as possible. After the first stage is conducted the far field energy is approximated by the monopole approximation and by a Cartesian energy expansion of first and second order with respect to the particle positions relative to the box centers to incorporate monopole and dipole contributions. In addition we have taken into account contributions of higher order to compute the far field energy for particle systems with high symmetry as accurate as possible. The near field energy is always computed before the second stage is carried out. In case a relative energy error is specified the computation of the corresponding absolute error is more accurate compared to the first stage.

The constants used in the error estimation scheme have to be computed separately for each value of the FMM separation criterion ws. We have implemented a procedure to minimize the computation time with respect to the separation in the near and far field part. Using this procedure we have always obtained the best runtime behavior for the separation criterion $ws=1$. The increase in the total runtime as a consequence of our error estimation scheme is negligible because most of the necessary data is precomputed and stored as

TABLE XI. Comparison of relative errors of two FMM calculations, one with use of the operator **C** (local-to-local translation) and the second one without for single, double, and quadruple precision. The threshold ϵ depends on the length of the mantissa in the binary floating point representation.

ϵ	Δ_1	Δ_2	Δ_3	Δ_4
$2^{-23} \approx 1.192 \times 10^{-07}$	2.019×10^{-07}	1.192×10^{-07}	8.241×10^{-07}	1.289×10^{-03}
$2^{-52} \approx 2.220 \times 10^{-16}$	7.521×10^{-16}	2.220×10^{-16}	1.717×10^{-15}	5.773×10^{-08}
$2^{-112} \approx 1.926 \times 10^{-34}$	3.262×10^{-34}	1.926×10^{-34}	1.005×10^{-33}	1.558×10^{-26}

constants in a library. Our scheme can easily be modified to treat a user-requested threshold with respect to an absolute error bound for the components of the potential or the gradient. Therewith it gives the possibility to specify up to three different thresholds, one for the energy, a second one for the components of the potential, and another one for the components of the gradient. In case the FMM is extended to other potentials or periodic boundary conditions (subject of a next paper) our error estimation scheme can easily be adapted.

Finally it should be noted, that the equations we have presented are mathematical representations of the method and potentially not the most computationally efficient.

APPENDIX A: FMM NOTATION

Our mathematical representation of the FMM is based on the notation used by White and Head-Gordon.[4,5] We consider two separated boxes (Fig. 1). The multipole moments of the boxes are defined as follows:

$$\omega_{lm}^{\text{box } 1} = \sum_{I=1}^{N^{\text{box } 1}} q_I a_I^l \frac{1}{(l+m)!} P_{lm}(\cos(\alpha_I)) e^{-im\beta_I} \tag{A1}$$

and

$$\omega_{jk}^{\text{box } 2} = \sum_{J=1}^{N^{\text{box } 2}} q_J a_J^j \frac{1}{(j+k)!} P_{jk}(\cos(\alpha_J)) e^{-ik\beta_J}. \tag{A2}$$

The upper bounds $N^{\text{box } 1}$ and $N^{\text{box } 2}$ represent the numbers of particles in the boxes. q_I and q_J are the charges of particle I in box 1 and particle J in box 2, respectively. a_I, α_I, and β_I as well as a_J, α_J, and β_J define the particle positions with respect to the box centers. The energy is given by

$$\begin{aligned} E &= \sum_{l=0}^{\infty} \sum_{m=-l}^{l} \sum_{j=0}^{\infty} \sum_{k=-j}^{j} (-1)^j \omega_{lm}^{\text{box } 1} B_{j+l,\ k+m}(\mathbf{R}_2 - \mathbf{R}_1) \omega_{jk}^{\text{box } 2} \\ &= \sum_{l=0}^{\infty} \sum_{m=-l}^{l} \sum_{j=0}^{\infty} \sum_{k=-j}^{j} (-1)^l \omega_{lm}^{\text{box } 2} B_{j+l,\ k+m}(\mathbf{R}_2 - \mathbf{R}_1) \omega_{jk}^{\text{box } 1} \end{aligned} \tag{A3}$$

with

$$B_{j+l,\ k+m} = \frac{1}{R^{j+l+1}} (j+l-k-m)! P_{j+l,\ k+m}(\cos(\theta)) e^{i(k+m)\phi},$$

$$R = \sqrt{(x_2-x_1)^2 + (y_2-y_1)^2 + (z_2-z_1)^2}, \quad \cos(\theta) = \frac{z_2 - z_1}{R}, \tag{A4}$$

$$\cos(\phi) = \begin{cases} \dfrac{x_2 - x_1}{\sqrt{(x_2-x_1)^2 + (y_2-y_1)^2}}, & \cos^2(\theta) < 1 \\ 1, & \cos^2(\theta) = 1, \end{cases}$$

$$\sin(\phi) = \begin{cases} \dfrac{y_2 - y_1}{\sqrt{(x_2-x_1)^2 + (y_2-y_1)^2}}, & \cos^2(\theta) < 1 \\ 0, & \cos^2(\theta) = 1. \end{cases}$$

The elements of operator **B** satisfy the condition

$$B_{j+l,\ k+m}(\mathbf{R}_1 - \mathbf{R}_2) = (-1)^{j+l} B_{j+l,\ k+m}(\mathbf{R}_2 - \mathbf{R}_1). \tag{A5}$$

In comparison to the notation used by White and Head-Gordon[4,5] we write the operator **B** as a double subscripted array. The spherical coordinates R, θ, and ϕ depend on the relative position of the two box centers represented by $\mathbf{R}_1 = (x_1, y_1, z_1)^T$ and $\mathbf{R}_2 = (x_2, y_2, z_2)^T$ to each other. Now we can define Taylor coefficients for the two boxes

$$\mu_{lm}^{\text{box } 1} = \sum_{j=0}^{\infty} \sum_{k=-j}^{j} (-1)^j B_{j+l,\ k+m}(\mathbf{R}_2 - \mathbf{R}_1) \omega_{jk}^{\text{box } 2} \tag{A6}$$

and

TABLE XII. The utilization of precision increase of the binary floating point representation. The relative errors of energies, potential, and gradient decrease in the same manner as the length of the mantissa increases from 52 (double precision ε_d) to 112 (quadruple precision ε_q).

$\left(\frac{\epsilon_q}{\epsilon_d}\right)$	$\frac{\Delta_1(\epsilon_q)}{\Delta_1(\epsilon_d)}$	$\frac{\Delta_2(\epsilon_q)}{\Delta_2(\epsilon_d)}$	$\frac{\Delta_3(\epsilon_q)}{\Delta_3(\epsilon_d)}$	$\frac{\Delta_4(\epsilon_q)}{\Delta_4(\epsilon_d)}$
$2^{-60} \approx 8.674 \times 10^{-19}$	4.337×10^{-19}	8.674×10^{-19}	5.849×10^{-19}	2.698×10^{-19}

$$\mu_{lm}^{\text{box }2} = \sum_{j=0}^{\infty} \sum_{k=-j}^{j} (-1)^l B_{j+l,\ k+m}(\mathbf{R}_2 - \mathbf{R}_1)\omega_{jk}^{\text{box }1}. \tag{A7}$$

The multipole moments and the Taylor coefficients can be combined to compute the energy

$$E = \sum_{l=0}^{\infty} \sum_{m=-l}^{l} \omega_{lm}^{\text{box }1}\mu_{lm}^{\text{box }1} = \sum_{l=0}^{\infty} \sum_{m=-l}^{l} \omega_{lm}^{\text{box }2}\mu_{lm}^{\text{box }2}$$

$$= \frac{1}{2}\sum_{l=0}^{\infty} \sum_{m=-l}^{l} (\omega_{lm}^{\text{box }1}\mu_{lm}^{\text{box }1} + \omega_{lm}^{\text{box }2}\mu_{lm}^{\text{box }2}). \tag{A8}$$

The multipole moments and the Taylor coefficients can be translated in space by using the operators **A** and **C**, respectively.[4,5] The rotation based FMM[4,5] reduces the $\mathcal{O}(p^4)$ scaling to $\mathcal{O}(p^3)$. In our FMM implementation the elements of operator **B** range from B_{00} to $B_{2p,\,2p}$.

[1] L. F. Greengard and V. Rokhlin, J. Comput. Phys. **73**, 325 (1987).
[2] L. F. Greengard, *The Rapid Evaluation of Potential Fields in Particle Systems* (MIT Press, Cambridge, 1988).
[3] L. F. Greengard and V. Rokhlin, *The Rapid Evaluation of Potential Fields in Three Dimensions* (Springer Press, Berlin, Heidelberg, 1988).
[4] C. A. White and M. Head-Gordon, J. Chem. Phys. **101**, 6593 (1994).
[5] C. A. White and M. Head-Gordon, J. Chem. Phys. **105**, 5061 (1996).
[6] M. P. Allen and D. J. Tildesley, *Computer Simulation of Liquids* (Oxford University, Oxford, 1990).
[7] J. M. Dawson, Rev. Mod. Phys. **55**, 403 (1983).
[8] K. E. Schmidt and M. A. Lee, J. Stat. Phys. **63**, 1223 (1991).
[9] H. G. Petersen, E. R. Smith, and D. Soelvason, Proc. R. Soc. London, Ser. A **448**, 401 (1995).
[10] D. Sølvason and H. G. Petersen, J. Stat. Phys. **86**, 391 (1997).
[11] C. H. Choi, K. Ruedenberg, and M. S. Gordon, J. Comput. Chem. **22**, 1484 (2001).
[12] J. Purnell, E. M. Snyder, S. Wei, and A. W. Castleman, Chem. Phys. Lett. **229**, 333 (1994).
[13] T. Ditmire, T. Donnelly, A. M. Rubenchik, R. W. Falcone, and M. D. Perry, Phys. Rev. A **53**, 3379 (1996).
[14] T. Ditmire, J. W. G. Tisch, E. Springate, M. B. Mason, N. Hay, R. A. Smith, J. Marangos, and M. H. R. Hutchinson, Nature (London) **386**, 54 (1997).
[15] U. Saalmann and J. M. Rost, Phys. Rev. Lett. **91**, 223401 (2003).
[16] U. Saalmann, Ch. Siedschlag, and J. M. Rost, J. Phys. B **39**, R39 (2006).
[17] I. Kabadshow and H. Dachsel, The Fast Multipole Method (http://www.fz-juelich.de/jsc/fmm/).
[18] B. C. Carlson and G. S. Rushbrooke, Proc. Cambridge Philos. Soc. **46**, 626 (1950).
[19] A. R. Edmonds, *Angular Momentum in Quantum Mechanics* (Princeton University Press, Princeton, 1957).
[20] H. Dachsel, J. Chem. Phys. **124**, 144115 (2006).
[21] P. McCabe, J. N. L. Connor, and D. Sokolovski, J. Chem. Phys. **114**, 5194 (2001).